Prefrontal Cortex Afferents to the Anterior Temporal Lobe in the *Macaca fascicularis* Monkey

Alicia Mohedano-Moriano,[1] Mónica Muñoz-López,[1] Ernesto Sanz-Arigita,[2] Palma Pró-Sistiaga,[3] Alino Martínez-Marcos,[4] María Ester Legidos-Garcia,[1] Ana María Insausti,[5] Sandra Cebada-Sánchez,[1] María Del Mar Arroyo-Jiménez,[1] Pilar Marcos,[1] Emilio Artacho-Pérula,[1] and Ricardo Insausti[1]*

[1]Department of Health Sciences, University of Castilla–La Mancha, Albacete 02006, Spain
[2]Radiology and Image Analysis Center - Free University Medical center (VUmc), Amsterdam, The Netherlands
[3]UNICAEN, UMS 3408, GIP Cyceron, Campus Jules Horowiz, 1474, Caen, France
[4]Department of Health Sciences, University of Castilla–La Mancha, Ciudad Real, 13071, Spain
[5]Department of Health, Physical Therapy School, Public University of Navarre, Tudela Campus, 31005, Tudela, Spain

ABSTRACT

The anatomical organization of the lateral prefrontal cortex (LPFC) afferents to the anterior part of the temporal lobe (ATL) remains to be clarified. The LPFC has two subdivisions, dorsal (dLPFC) and ventral (vLPFC), which have been linked to cognitive processes. The ATL includes several different cortical areas, namely, the temporal polar cortex and rostral parts of the perirhinal, inferotemporal, and anterior tip of the superior temporal gyrus cortices. Multiple sensory modalities converge in the ATL. All of them (except the rostral inferotemporal and superior temporal gyrus cortices) are components of the medial temporal lobe, which is critical for long-term memory processing. We studied the LPFC connections with the ATL by placing retrograde tracer injections into the ATL: the temporal polar ($n = 3$), perirhinal (areas 35 and 36, $n = 6$), and inferotemporal cortices (area TE, $n = 5$), plus one additional deposit in the posterior parahippocampal cortex (area TF, $n = 1$). Anterograde tracer deposits into the dLPFC (A9 and A46, $n = 2$), the vLPFC (A46v, $n = 2$), and the orbitofrontal cortex (OF; $n = 2$) were placed for confirmation of those projections. The results showed that the vLPFC displays a moderate projection to rostral area TE and the dorsomedial portion of the temporal polar cortex; in contrast, the dLPFC connections with the ATL were weak. By comparison, the OFC and medial frontal cortices (MFC) showed dense connectivity with the ATL, namely, A13 with the temporopolar and perirhinal cortices. All areas of the MFC projected to the temporopolar cortex, albeit with a lower intensity. The functional significance of such paucity of LPFC afferents is unknown. J. Comp. Neurol. 523:2570–2598, 2015.

INDEXING TERMS: prefrontal cortex; anterior temporal cortex; afferents; nonhuman primate

The human and nonhuman primate prefrontal cortex has three main portions that cover the lateral (lateral prefrontal cortex [LPFC]), medial (medial prefrontal cortex [MFC]), and basal (orbital) aspects of the frontal lobe (prefrontal orbital cortex [OFC]). The LPFC can be divided into the dorsolateral prefrontal cortex (dLPFC) and ventrolateral prefrontal cortex (vLPFC) in nonhuman primates according to different cytoarchitectonic and connectivity studies (Walker, 1940; Barbas and Pandya, 1989; Carmichael and Price, 1994; Petrides and Pandya, 1999, 2002; Saleem et al., 2007, 2014; Luebke et al., 2010; Petrides et al., 2012). Functional studies in humans (Tanji and Hoshi, 2008; Bonnici et al., 2012; Petrides et al., 2012; Takahashi et al., 2013) also support this division. The dLPFC is the cortex located dorsal to the upper bank of the principal sulcus (ps) and encompasses Brodmann's areas 9, 8, and the portion of area 46 that lies above the ps. The dLPFC, receives projections from the parietal cortex, which is involved in visuospatial location (Corbetta et al., 1998; Muñoz and Evering, 2004; Petrides and Pandya, 2009). The

The first two authors contributed equally to most of the research.

Grant sponsor: Ministry of Education, Science and Technology and Innovation, Spain; Grant numbers: PM92-0166, BFI 2000-0418, BFI2003-09581, BFU 2006-12964, BFU 2009-14705.

*CORRESPONDENCE TO: Ricardo Insausti, Department of Health Sciences, University of Castilla–La Mancha, Almansa 14, 02006 Albacete, Spain. E-mail: ricardo.insausti@uclm.es

Received August 10, 2014; Revised November 30, 2014;
Accepted April 29, 2015.
DOI 10.1002/cne.23805
Published online July 7, 2015 in Wiley Online Library (wileyonlinelibrary.com)

vLPFC is located ventral to the ps, and comprises Brodmann's areas, 45, 12l, and the portion of area 46 ventral to the ps. The vLPFC receives projections primarily from the unimodal visual cortex (Hoshi, 2006; Tanji and Hoshi, 2008). LPFC functional activity is associated with executive functions and working memory (Fuster and Alexander, 1971; Goldman-Rakic, 1992; Funahashi, 2006). The OFC is made up of Brodmann's areas 10, 11, and 13 (Walker, 1940), as well as 12o (Carmichael and Price, 1994), and other general divisions (Barbas and Pandya, 1989; Morecraft et al., 1992). The MFC Brodmann's areas 25, 32, and 24 (Barbas and Pandya, 1989; Carmichael and Price, 1994) complete the medial prefrontal cortex.

The anterior temporal lobe (ATL) is an ill-defined area that comprises several anatomically and functionally diverse cortical areas (Benevento, 1977; Desimone and Gross, 1979; Bruce et al., 1981; Baylis et al., 1987; Jellema et al., 2004; Saleem et al., 2007). Under the term ATL we include the temporal polar cortex (TPC), the rostralmost portion of the perirhinal cortex (PRC; areas 35 and 36 of Brodmann, 1909) at the transition with area TE, as far as the tip of the superior temporal sulcus (sts), including the anterior limit of the superior temporal gyrus (STG). Whereas the anterior limit of the ATL is the temporal pole, the caudal limit is approximately located at the beginning of the amygdala. This location corresponds to levels +25 of Szabo and Cowan (1984) in the *Macaca fascicularis* monkey, and +19.65 of Paxinos et al. (2000) and +22 of Saleem and Logothetis (2012) in *Macaca mulatta*. Therefore, the ATL extends caudal to the tip of the temporal pole for about 5 mm in *Macaca fascicularis* monkey, and 6 mm in the *Macaca mulatta* brain.

Physiologically, Desimone and Gross (1979) characterized a caudal portion of area TE that presented large visual receptive fields, and a rostral portion, where neurons showed polymodal responses. In addition, auditory and visceral responses can be also found in the dorsolateral and dorsomedial part of the temporal pole, respectively (Kaada et al., 1949; Moran et al, 1987). Polymodal sensory responses were found in "the cortex dorsal, anterior and ventral to IT" (Desimone and Gross, 1979). Baylis et al. (1987) also described a small proportion of cells responsive to auditory and oral stimuli, in the anterior portion of area TE1 of Seltzer and Pandya (1978), in addition to more common visual stimuli responses. Memory-related responses have also been detected in zones of the ATL (Miyashita and Chang, 1988; Riches et al., 1991; Fahy et al., 1993; Miyashita et al., 1993; Nakamura and Kubota, 1995), including complex responses to visual stimuli, such as the detection of recency and familiarity (Desimone and Gross, 1979; Fuster and Jervey, 1981; Brown et al., 1987; Fahy et al., 1993; Miller et al., 1991, 1993; Miller and Desimone, 1994; Nakamura et al., 1994; Nakamura and Kubota, 1995).

Lesion studies in primates show that the ATL is involved in visual recognition memory (Horel et al., 1987; Phillips et al., 1988; Murray et al., 1989; Gaffan and Murray, 1992; Meunier et al., 1993; Zola-Morgan et al., 1993; Gaffan, 1994; Weller et al., 2006). Moreover, ATL lesions in humans and in nonhuman primates produce visual agnosia and complex behavioral deficits such as Klüver–Bucy syndrome (Klüver and Bucy, 1939; Olson, 2003). The anatomical and functional organization of the ATL, in particular the TPC, is still considered "enigmatic" (Olson et al., 2007). In addition, the ATL has been considered a "hub" for neuroanatomical pathways involved in semantic memory processing, as damage to the ATL is present in frontotemporal or semantic dementia in humans (Patterson et al., 2007; Binney et al., 2010). Further evidence derives from functional studies in humans that show an activation of cortical areas within the ATL, ventromedial prefrontal cortex (areas 14 and 25), as well as the hippocampus during encoding, consolidation, and retrieval of old memories related to recent and remote memories (Bonnici et al., 2012; Van Kesteren et al., 2012).

The anatomical connection of the ATL and prefrontal cortex via the uncinate fasciculus has been known since the beginning of the last century (Curran, 1909; Klüver and Bucy, 1939; Nauta and Whitlock, 1956; Kaada, 1960; Klingler and Gloor, 1960). However, whereas the current anatomical literature deals mainly with the OFC and MFC connectivity with the ATL, the available information about dLPFC and vLPFC connectivity is related to executive and visuomotor associations (Selemon and Goldman-Rakic, 1988; Petrides and Pandya, 1984; Fuster, 2008; Gerbella et al., 2010; Borra et al., 2011). It is well known that parts of the temporal lobe caudal to the ATL as well as the parietal cortex, mainly area 7, provide afferents to both the dLPFC and vLPFC (Petrides and Pandya, 1984, 2009; Cavada and Goldman-Rakic, 1989). In addition, the premotor cortex, mainly fields F6 and F7 (Luppino et al., 1993; Rizzolatti and Luppino, 2001) and the retrosplenial cortex (Goldman-Rakic et al., 1984; Morris et al., 1999; Kobayashi and Amaral, 2007; Yeterian et al., 2012). complete the set of connections.

The afferents of the MFC and OFC to the temporal lobe have been extensively studied, starting from degeneration tracing studies (Pandya and Kuypers, 1969; Jones and Powell, 1970; Van Hoesen et al., 1975; Van Hoesen and Pandya, 1975). Retrograde and anterograde tracing techniques refined and revealed

additional details of such connectivity (Kawamura and Naito, 1984; Markowitsch et al., 1985; Moran et al., 1987; Shiwa, 1987; Barbas, 1988, 1993; Petrides and Pandya, 1988; Seltzer and Pandya, 1989; Ungerleider et al., 1989; Ban et al., 1991; Martin-Elkins and Horel, 1992; Morecraft et al., 1992; Distler et al., 1993; Arikumi et al., 1994; Rodman, 1994; Rodman and Consuelos, 1994; Suzuki and Amaral, 1994a; Webster et al., 1994; Carmichael and Price, 1995; Cavada et al., 2000; Janssen et al., 2000; Lavenex et al., 2002; Kondo et al., 2003, 2005; Insausti and Amaral, 2008; Saleem et al., 2014). This projection is also present in other primate species, such as the owl monkey (Weller and Kaas, 1987) and the squirrel monkey (Weller and Steele, 1992).

Data from the reports mentioned above suggest that only cortical regions caudal to the ATL present a sizeable projection to the LPFC. A knowledge of the dLPFC and vLPFC anatomical relationship with the ATL would be of interest in dealing with a possible influence on the MTL, and very likely on memory processing. Indeed, the ATL is broadly coincident with the "hub" area where convergence for sensory processing takes place (Patterson et al., 2007), which might also be related to semantic memory and recognition memory. The particular convergence of multiple sensory modalities in the ATL prompted us to analyze the afferent connectivity to the ATL from the LPFC with anatomical tracing techniques. The question of the extent and density of the connections of the ATL with the LPFC needs to be defined more precisely. This connectivity is also compared with the much better known anatomical relationship of the ATL with the OFC and MFC.

MATERIALS AND METHODS

Nineteen male *Macaca fascicularis* from R.C. Harstelust (Tilburg, The Netherlands) were used in the present study. Animals with a weight approximately of 3 kg at the time of surgery were housed individually. All experimental procedures were carried out according to guidelines of the European Community on the welfare of research animals (directive 86/609/EEC, updated in 2010/63 EU), after approval and supervision by the local Ethics Committee for Animal Research.

A 12-hour-fasting period preceded surgery. Animals were tranquilized with 8 mg/kg i.m. ketamine hydrochloride (Ketolar, Parke-Davis, Barcelona, Spain). Anesthesia level was maintained with 30 mg/kg i.v. Midazolam (Dormicum, Roche, Madrid, Spain)

Abbreviations

8	area 8 of Brodmann
9	area 9 of Brodmann
10	area 10 of Brodmann
11	area 11 of Brodmann
12	area 12 of Brodmann
12l	area 12, lateral portion
12o	area 12, orbitofrontal portion
13	area 13 of Brodmann
14	area 14 of Brodmann
24	area 24 of Brodmann
25	area 25 of Brodmann
32	area 32 of Brodmann
35	area 35 of Brodmann
35d	area 35 of Brodmann, dorsal portion
36	area 36 of Brodmann
36r	area 36 of Brodmann, rostral portion
36c	area 36 of Brodmann, caudal portion
38	area 38 of Brodmann
45	area 45 of Brodmann
46	area 46 of Brodmann
46d	area 46 of Brodmann, dorsal portion
46v	area 46 of Brodmann, ventral portion
A	amygdala
AA	^{3}H amino acids
ABC	avidin–biotin complex
amts	anterior middle temporal sulcus
ATL	anterior temporal lobe
as	arcuate sulcus
BDA	biotin dextran amine
cc	corpus callosum
cs	cingular sulcus
DAB	diaminobenzidine tetra-hydrochloride
dLPFC	lateral prefrontal cortex, dorsal portion
DY	diamidino yellow
EC	entorhinal cortex
E_{LR}	entorhinal cortex, lateral rostral subfield
E_{O}	entorhinal cortex, olfactory subfield
E_{R}	entorhinal cortex, rostral subfield
FB	Fast Blue
HIP	hippocampus
ips	intraparietal sulcus
ITG	inferior temporal gyrus
los	lateral orbital sulcus
LPFC	lateral prefrontal cortex
lus	lunate sulcus
mos	medial orbital sulcus
MFC	medial frontal cortex
MTL	medial temporal lobe
ois	inferior occipital sulcus
OFC	orbitofrontal cortex
OT	olfactory tubercle
PHR	parahippocampal region
Pir	piriform cortex
pmts	posterior middle temporal sulcus
Pro	proisocortex of Pandya and Sanides (1973)
ps	principal sulcus
PFC	prefrontal cortex
PPH	posterior parahippocampal cortex
PRC	perirhinal cortex
rs	rhinal sulcus
STG	superior temporal gyrus
STGf	superior temporal gyrus, fundus division
STGi	superior temporal gyrus, intermediate division
STGm	superior temporal gyrus, medial division
STGo	superior temporal gyrus, opercular division
STGr	superior temporal gyrus, radial division
sts	superior temporal sulcus
TB	Tris buffer
TBS	saline Tris buffer
TE	area TE of Von Bonin and Bailey (1947)
TE1	area TE1 of Seltzer and Pandya (1978)
TEa	area TEa of Seltzer and Pandya (1978)
TEad	dorsal subregion of anterior area TE
TEav	ventral subregion of anterior area TE
TF	area TF of von Bonin and Bailey (1947)
TH	area TH of von Bonin and Bailey (1947)
TPC	temporal polar cortex
TPCm	temporal polar cortex, medial portion
TPCl	temporal polar cortex, lateral portion
vLPFC	lateral prefrontal cortex, portion ventral
WGA–HRP	wheat germ agglutinin conjugated to horseradish peroxidase

supplemented as required. Surgery was carried out under aseptic conditions; heart rate, blood pressure, and rectal temperature were monitored. Animals were placed in a Kopf stereotaxic apparatus (Tujunga, CA), and a craniectomy was performed over the targeted cortical area for tracer injections. Prior to the opening of the dura mater, 20 ml of a 20% solution of mannitol (Apiroserum®, Antibióticos Farma, Madrid, Spain) was administered. Once the cortical area was exposed, tracers were injected with a Hamilton syringe at a depth of 1.5–2 mm under the pial surface. The volume injected was of 1 μl for the retrograde tracers (Fast Blue [FB], 3%; Diamidino Yellow [DY], 1%; Sigma, St. Louis, MO) and 2 μl for the anterograde tracer (biotinylated dextran amine [BDA], 10.000 MW, lysine fixable, 10%; Molecular Probes, Eugene, OR) as described previously (Muñoz and Insausti 2005; Mohedano-Moriano et al., 2008). Four cases were injected with a 1% solution of wheat germ agglutinin conjugated to horseradish peroxidase (WGA–HRP): 50–250 nl of WGA–HRP solution were slowly injected by means of short pulses of air (with a Picospritzer, General Valve, Fairfield, NJ) over a period of 20 minutes. Finally, one case, IM-12 (kindly provided by Dr. David G. Amaral, University of California, Davis and the MIND Institute, UC Davis), had a ^{3}H-amino acid injection in the OFC. Briefly, an equal amount of ^{3}H-leucine and ^{3}H-proline (L-[4-5-^{3}H] leucine; L-[2, 3-^{3}H] proline, respectively, New England Nuclear/Dupont, Wilmington, DE), vacuum-evaporated and reconstituted to a final concentration of 100 μC/μl, was injected (see Cowan et al., 1972 and Insausti and Amaral, 2008 for details).

After a period of 48 hours for WGA-HRP, or 14 days for fluorescent tracers and BDA, animals were tranquilized with ketamine (8 mg/kg i.m.), deeply anesthetized with sodium thiopental (200 mg/kg, sodium thiopenthal, Abbott, West Berkshire, UK), and perfused transcardially. Fixation was begun with 1% paraformaldehyde in 0.1 M phosphate buffer (pH 7.2, at a rate of 250 ml/min for 2 minutes) at room temperature followed by cold 4% paraformaldehyde in 0.1 M phosphate buffer (pH 7.2, 250 ml/min for 10 minutes), followed by 100 ml/min for 50 minutes, and finalized with 5% sucrose in 0.1 M phosphate buffer (4°C, pH 7.2, 100 ml/min for 20 minutes). Animals with injections of WGA–HRP were perfused according to Insausti et al. (1987). The head was placed on the stereotaxic frame, and the brain was blocked in the coronal plane. The brain was removed and photographed, and the blocks were then cryoprotected in a solution of 10% glycerol and 2% dimethylsulfoxide in 0.1 M phosphate buffer for 24 hours, followed by 20% glycerol and 2% dimethylsulfoxide in 0.1 M phosphate buffer for 48 hours. Blocks were subsequently sectioned in the coronal plane (50 μm thick) using a sliding microtome coupled to a freezing unit (Microm, Heidelberg, Germany) in series every 250 μm (five sections). One out of five series of sections was stained with thionin for cytoarchitectonic analysis; one adjacent section was immediately mounted for fluorescence analysis. In WGA–HRP experiments, one series of sections was processed according to Mesulam's protocol for histochemical demonstration of WGA–HRP transport as described (Insausti et al., 1987). BDA-labeled fibers were visualized as follows: first, the endogenous peroxidase activity was quenched by a 30-minute step in 0.03% H_20_2 in Tris-buffered saline (TBS; 50 mM, pH 7.6). Sections were then incubated for 2 hours in avidin–biotin complex (ABC Elite Kit, Vector, Burlingame, CA) at a working dilution of 1:200, diluted in Tris buffer (TB; 50 mM, pH 8.0) with 0.3% Triton X-100, finally reacted with 0.02% 3, 3′diaminobenzidine (DAB;, Sigma) in TB (pH 8.0) as chromogen, and intensified with nickel ammonium sulfate (0.4%) and H_20_2 (0.01%). The remaining sections were stored at −20°C in a cryoprotectant solution of 20% glycerol, 30% ethylene glycol, and phosphate buffer 0.05 M (pH 7.2) for future use.

The distribution of retrogradely labeled cells was analyzed with a microscope (Olympus BX50) provided with epifluorescence illumination and an ultraviolet filter (U-MWB2, 460–490 nm excitation; Olympus, Tokyo, Japan). The distribution of labeled neurons was charted with an X–Y charting system (AccuStage Minnesota Datametrics, St. Paul, MN). Anterograde labeling of BDA was charted by using a drawing tube at 20× magnification. Adjacent thionin-stained series were used for cytoarchitectonic analysis to define areal boundaries. The drawings in this study were prepared in Canvas 10.0 (Deneba, Miami, FL), and microphotographs were only adjusted for brightness and contrast using Adobe (San Jose, CA) Photoshop 7.0 (in Windows).

Two-dimensional, unfolded maps were constructed to represent the topography of the distribution of retrogradely labeled neurons. Details can be found in Insausti et al. (1987) and Muñoz and Insausti (2005).

Nomenclature

Cytoarchitectonic boundaries were based on previous descriptions, namely, that of Amaral et al. (1987) for the entorhinal cortex and Insausti et al. (1987) for the ATL cortex divisions of the upper bank of the sts. Area TE was subdivided according to the nomenclature of Seltzer and Pandya (1978). Frontal lobe areas were defined according to the general scheme of Walker (1940) modified according to Barbas and Pandya (1989), Petrides and Pandya (1999, 2002), and Petrides

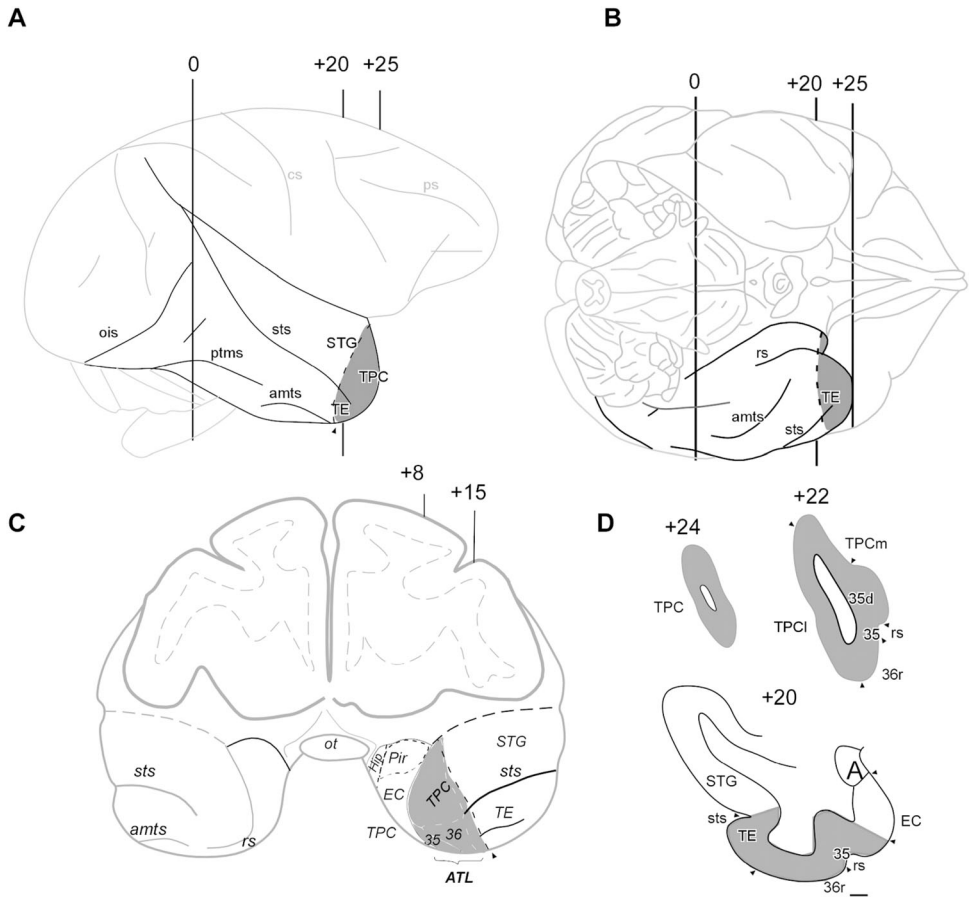

Figure 1. The approximate extent of the ATL in *Macaca fascicularis* is represente with depictions of the lateral (**A**), ventral (**B**) and frontal (**C**) surfaces of the brain, indicating the approximate extent of the ATL in stereotaxic coordinates (Szabo and Cowan, 1984). **D:** Coronal sections through the ATL with the approximate AP levels. For abbreviations, see list.

et al. (2012). We included area 12 of Walker (1940) as the strip of cortex that lies at the ventrolateral convexity that encompasses area 12l, the strip of cortex at the ventralmost portion of the lateral surface of the frontal lobe, and 12o, which extends into the lateral OFC as far as the lateral orbital sulcus (Petrides and Pandya, 2002). Other cortical areas such as area 14 (without labeling) were not subdivided (Petrides and Pandya, 2002). The TPC was divided as in Insausti (2013). Nomenclature of the PRC cortex and posterior parahippocampal cortex (PPH; areas TF and TH of von Bonin and Bailey, 1947) followed the description of Suzuki and Amaral (1994b, 2003).

The description of the limits established for the ATL is given in more detail in the following and in Figure 1. Classical cytoarchitectonic studies by Brodmann, (1909) divided the human temporal lobe into a temporopolar region (area 38) at the rostral limit of the superior and inferior temporal gyri. Areas 20, 21, and 22 continue at the dorsal and lateral aspects of the ATL. In the nonhuman primate, the rostral part of the ATL is clearly delimited by the temporal pole, but the caudal boundary is indistinct. Within the ATL, the cytoarchitectonic laminae of the monkey's temporal cortex become progressively less differentiated in a rostral direction, and the layering becomes less distinct. Rostral area TE has been separated into TEad (anterior–dorsal) and TEav (anterior–ventral) portions by Saleem and Tanaka (1996) based on anterograde tracer studies in *Macaca mulatta*. Figure 1 presents a diagram with the approximate extent of the ATL.

RESULTS

Injection sites

We used 15 retrograde tracer injections that included the TPC (n = 3), PRC (Brodmann's areas 35 and 36, n = 6), and rostral area TE (n = 5), PPH (n = 1), 6 anterograde tracer experiments, one with ^{3}H-amino acids in the OFC (contralateral side to the PPH retrograde tracer experiment), and 5 BDA prefrontal cortex deposits (Brodmann's areas 9, 46d, and 13, one case

TABLE 1.
Cases, Injection Site, and Tracer, and Tracer Used for Each

Case	Injection site	Tracer
M1-93	Temporal polar cortex	WGA-HRP
M3-93	Temporal polar cortex	WGA-HRP
M15-96	Temporal polar cortex	FB
M2-93	Perirhinal cortex A36r	WGA-HRP
M3-94	Perirhinal cortexA 35	DY
M4-94	Perirhinal cortex A36r	DY
M5-94	Perirhinal cortex A36r	DY
M5-94	Perirhinal cortex A36r	FB
M16-96	Perirhinal cortex A36c	FB
M6-93	Rostral TE1	WGA-HRP
M1-96	Rostral TE1	FB
M15-96	Rostral TE1	DY
M6-02	Rostral TEa	FB
M7-02	Rostral TEa	FB
M1-05	Rostral A9	BDA
M2-05	A46 (ventral)	BDA
M3-05	A46 (ventral)	BDA
M4-05	A46 (Dorsal)	BDA
M6-05	A13	BDA
IM-12	A13	AA
IM-12	TF	FB

For abbreviations, see list.

each) and 46v ($n = 2$). Table 1 presents the list of cases; Figures 2 and 3 show the deposit location in our experimental series. The relative amount of retrogradely labeled neurons is expressed as total number (Table 2A) and as a percentage of the total number of retrogradely labeled prefrontal neurons in representative cases in each of the experimental groups (Table 2B).

Frontal cortex afferents to the TPC based on retrograde tracer injections

Case M1-93 will be described in more detail among the cases with ventral injections in the TPC, as case M3-93 resulted in a smaller deposit (Figs. 2, 3C). Sparse retrograde label was observed in area 10 at very rostral levels (Fig. 4A,D). The dLPFC displayed a moderate amount of retrogradely labeled neurons (2%) at the midfrontal level, at the border of the lateral and medial aspects of the frontal lobe (M1-93, Fig. 4A,G). Neither area 46d nor area 8 presented retrogradely labeled neurons. The vLPFC presented a moderate-to-low number of labeled neurons in area 46v (1%, Fig. 4A,E,F) and area 12l (the number in the table results is 0%, although 40 neurons were found). This kind of numerical result is presented in all our cases: numbers lower than 0.5% are rounded to 0%. Table 2A shows the total number of retrogradely labeled neurons. Likewise, area 45 is 0% (20 neurons; Fig. 4A).

The OFC had a high density of retrogradely labeled neurons (Fig. 4A,E–I) that occupied most of the OFC transverse axis. At the rostral level of area 11, retrograde label reached up to 500 neurons per section (13%; an example of such labeling can be seen in Fig. 4A,E,F). This distribution of labeled neurons continued caudally for several mm and reached the rostral part of area 13. This area presented among the highest number of the total labeled neurons (74%; Fig. 4A,G–I). Area 12o yielded 1% of the total number of labeled cells (Fig. 4A,F–I). The majority of the retrogradely labeled neurons all over the OFC were in layer III, with fewer in layer V (Figs. 13C, 14C).

Caudally, retrogradely labeled neurons aggregated into four distinct broad patches, 1–2 mm wide separated by spaces devoid of labeled neurons, in a sort of longitudinally stripped pattern (Fig. 4I). The medial and most rostral patch occupied the medial portion of area 13 (Fig. 4A,H,I). This patch of label sometimes straddled over the lateral portion of area 14, and extended in a rostrocaudal direction, from the rostral limit of the corpus callosum, as far as to the olfactory tubercle (Fig. 4A). This patch (over 700 labeled neurons) had a longitudinal extension of 4 mm. The transverse extension was about 2 mm, and the number of labeled neurons reached up to 300 for a single patch (Fig. 4A). Such groups were located immediately rostral to the olfactory tubercle. At progressively more caudal levels, the bands of retrograde labeling fused, and formed a single band, increasing in density up to 1,000; this was the highest number of retrogradely labeled neurons found in all our experimental cases. This patch continued with the anterior insular cortex. Caudally, the total size of the cortical area covered by these patches was approximately 4 mm (length) by 2.5 mm (width), whereas at the rostral level the OFC labeling was continuous and much reduced in extent. Overall, the patches presented more labeled neurons in layer III than in layer V, although at points of maximal density, distributed in all layers, throughout the thickness of the cortex.

The MFC had retrogradely labeled neurons at the level of the anterior limit of the cingulate sulcus. Labeled neurons in rostral area 24 were observed in the ventral bank of the cingulate sulcus, at the rostral limit of the corpus callosum (2%; Fig. 4A,G–I), as well as close to the fundus of the cingulate sulcus (up to 40 labeled neurons). Smaller groups of labeled neurons were located in area 32 (1%; Fig. 4A,H) close to the rostral sulcus, and in the subcallosal area 25 (1%; Fig. 4A,I). The latter extended as far as the olfactory tubercle. Area 14 also contained 1% of labeled neurons, (Fig. 4A,G,H).

Retrograde labeling in the MFC was concentrated mainly in layer III. The overall distribution of the labeling in this case is represented in the unfolded map shown in Figure 4A.

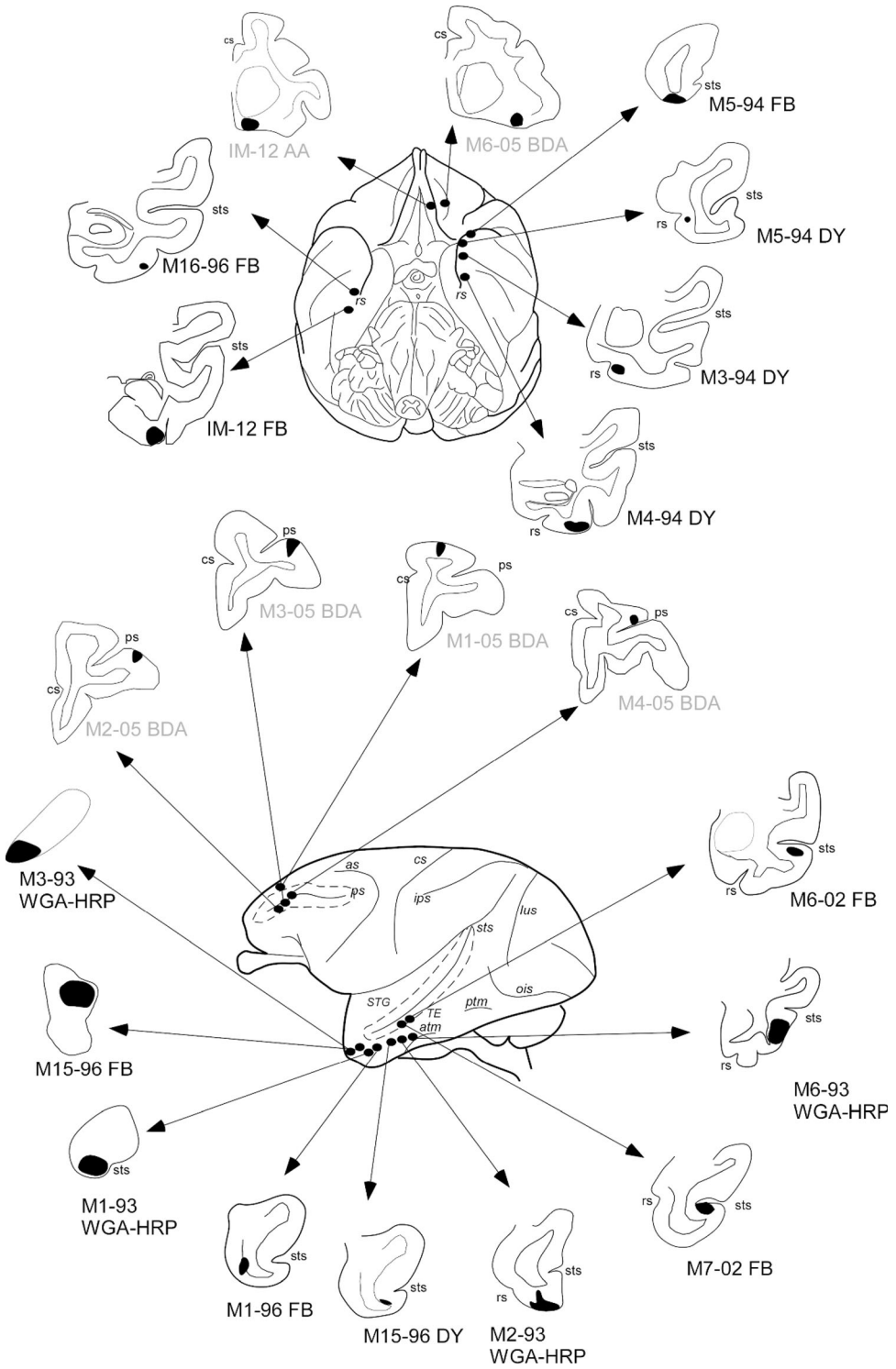

Figure 2. Anterograde and retrograde tracer deposits in this study are represented on the cortical surface of the *Macaca fascicularis*. The TPC, PRC (areas 35 and 36r), and rostral area TE of the inferotemporal cortex had retrograde tracers deposits, all placed in the left hemisphere (for clarity, IM-12 FB, and M-16-96 FB are represented on the right-hand side of the figure). Additional deposits in area 36c and PPH are indicated. The anterograde tracer deposits in the dLPFC, vLPFC, and OFC of the PFC (areas 9, 46, and 13) are indicated in gray lettering. For abbreviations, see list.

Case M3-93 had a much smaller injection of WGA–HRP, aimed at the same place as in experiment M1-93, described above (Fig. 2). The injection site was slightly ventral and lateral compared with M1-93. Although the results replicated case M1-93, the labeling was much more limited. As in experiment M1-93, the dLPFC had

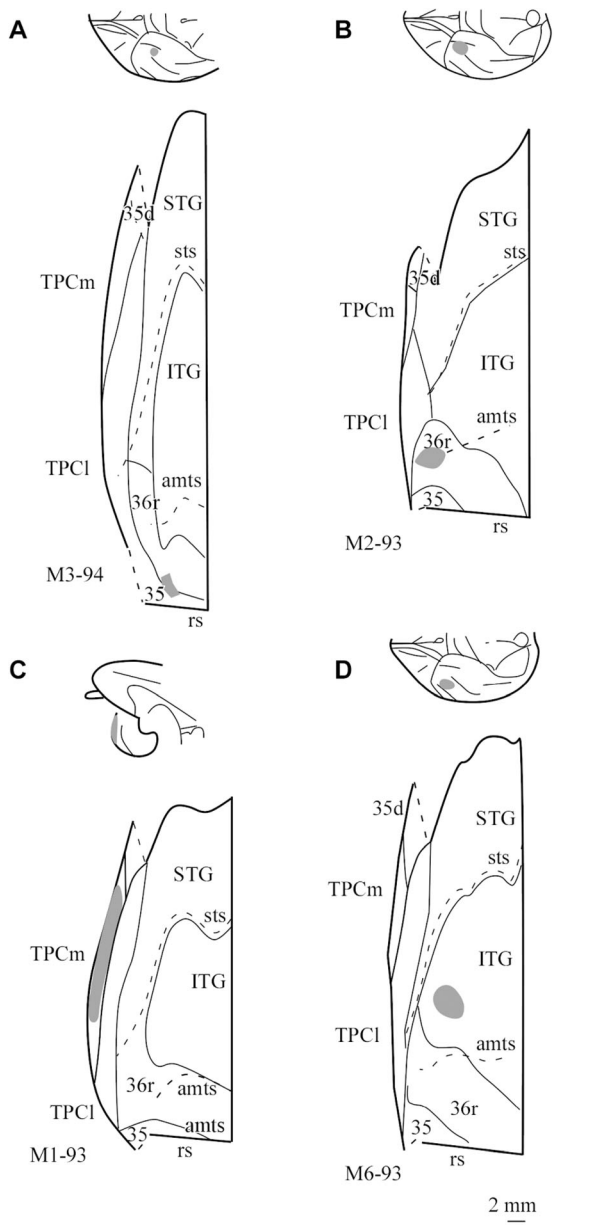

Figure 3. Two-dimensional map reconstruction of tracer deposit extent in four representative cases: (**A**) injection in area 35 of the PRC; (**B**) injection in area 36r of the PRC; (**C**), injection in the TPC; (**D**) injection in area TE1 of the rostral inferotemporal cortex. On each panel, the upper figurine shows the location of deposits on the brain surface. For abbreviations, see list. Scale bar = 2 mm in D (applies to A–D).

an isolated patch (just a few labeled neurons) in caudal area 8 (Fig. 5A). In contrast, no labeled neurons were present in other parts of the vLPFC. Patches of retrogradely labeled neurons were found in the OFC, starting at the caudal limit of area 11 and extending into area 13, close to the medial orbital sulcus. Rostral area 12o had a patch of labeled neurons at only a single level. In caudal area 13, labeled neurons formed single, isolated clumps of neurons, lateral to the olfactory tubercle. In all these locations, layer III was predominantly labeled.

Case M15-96 had an FB deposit that extended to all layers of the dorsal and medial part of the temporal pole (Fig. 2). A few scattered neurons, were present in area 9 (1%) as well as in the rostralmost portion of area 46d (0%, six labeled neurons; Fig. 5B). Scattered neurons were found in the rostral one-fourth of the ventral lip of the ps (46v of vLPFC, 2%). Moreover, area 12l had 0% (only three labeled neurons). OFC labeling showed a total of 1%, located in area 11. Area 12o yielded up to 2% of the total. An overall representation of the labeling in this case is presented in Figure 5B. A moderate to light density of neurons was found in area 13 (14% of the OFC). This case showed a high density of retrogradely labeled neurons in areas of the MFC such as areas 10 (12%), 24 (15%), 32 (16%), and area 25 (subcallosal area, 14%). Area 14 presented abundant retrograde labeling in the ventral MFC (23%), at the vertex of the medial and ventral aspects of the frontal lobe. Although the vast majority of labeled neurons were located in the MFC, some neurons were also found in other parts of the frontal cortex.

In summary, the results after tracer injections into the temporal pole showed that LPFC labeling after injections into the dorsal part of the temporal pole was more abundant than injections in its ventral part. The deposit into the dorsal part of the temporal pole labeled neurons (albeit in low numbers) in the dLPFC, area 9 (1%), area 46d (0%, six labeled neurons), and the vLPFC (12l, 0%; 46v, 2%), which was different from the deposits in the ventral part of the temporal pole (areas 46v, 1%; 12 and 45, 0%). Whereas the dorsal part of the temporal pole received dense projections from the MFC (68%), and moderate projections from the OFC (17%), the ventral injection presented projections almost exclusively from the OFC (88%; Fig. 13A,C), and much less from the MFC (5%).

Frontal cortex afferents to the PRC based on retrograde tracer injections

One injection was placed in area 35 (M3-94 DY). Area 36r was injected in four cases (M2-93 WGA–HRP, M4-94 DY, M5-94 DY, and M5-94 FB), and area 36c in one case (M16-96 FB). The latter extended slightly into the adjacent portion of area 36.

Case M3-94 had a rather small deposit of DY largely confined to area 35 at the level of the rostral part of the amygdaloid complex, lateral to the rhinal sulcus (Figs. 2, 3A). No retrograde label was observed in the dLPFC or vLPFC (Fig. 6A). Area 12l had no labeled neurons, whereas area 12o presented a total percentage

TABLE 2.

Retrogradely Labeled Neurons (total number [A] and % [B]) in Representative Cases in Each Experimental Group.

A) Labeled cells								
	Temporal pole		Perirhinal cortex		Inferotemporal cortex			
Area/case	M1-93	M15-96FB	M3-94DY	M2-93	M6-93	M15-96DY	M7-02FB	M6-02FB
A10	360	153	0	140	0	0	0	0
A8	0	0	0	0	0	0	0	6
A9	180	12	0	3	0	0	9	27
A46d	0	6	0	0	0	0	15	0
A46v	80	27	0	0	140	35	124	31
A45	20	0	0	0	280	93	48	70
A12l	40	3	0	0	440	3	165	78
A12o	60	26	220	0	200	21	465	112
A11	1,200	15	0	0	20	0	572	68
A13	6,700	172	640	560	1,260	70	677	127
A14	120	284	0	0	20	0	6	43
A25	80	169	0	0	20	0	0	0
A32	60	197	0	40	0	0	6	0
A24	160	185	0	20	20	0	6	18
Total labeled neurons	9,060	1,249	860	763	2,400	222	2,093	580
B) % of labeled neurons								
A10	4	12	0	18	0	0	0	0
A8	0	0	0	0	0	0	0	1
A9	2	1	0	0	0	0	0	5
A46d	0	0	0	0	0	0	1	0
A46v	1	2	0	0	6	16	6	5
A45	0	0	0	0	12	42	2	12
A12l*	0	0	0	0	18	1	8	13
A12o*	1	2	26	0	8	9	22	19
A11	13	1	0	0	1	0	27	12
A13	74	14	74	73	53	32	32	22
A14	1	23	0	0	1	0	0	7
A25	1	14	0	0	1	0	0	0
A32	1	16	0	5	0	0	0	0
A24	2	15	0	3	1	0	0	3

(26%) as a patch located at the border with the orbital surface of the frontal lobe, adjacent to area 13. The caudal part of area 13 contained most of the labeling (up to 20 in a single section) at the center of the caudal part of area 13 (total percentage 74%; Fig. 6A,F,G). Layer III had the most labeled neurons.

The largest deposit in area 36r was in case M2-93 (Figs. 2, 3B); this will be described in more detail. Case M2-93 had small amounts (up to five labeled neurons per section) in layer III of the rostral portion of area 10 (18%; Fig. 7A,D). Occasional neurons were observed in rostral area 9 (0%, three neurons; Fig. 7A). No other labeling was seen in any other part of the LPFC. No labeled neurons were observed in the OFC except in the caudal portion of area 13 (73%; Fig. 7A,H,I), where a small number (5–10) of retrogradely labeled pyramidal neurons in layer III were found, in between the medial and lateral orbital sulci (Fig. 7H). The MFC (areas 24, 3%; and 32, 5%) accounted for 8% (Fig. 7A,F,G). The characteristics of the tracer deposit in M2-93, which involved mostly the superficial layers of the cortex, resulted in a lower number of retrogradely labeled neurons in the orbitofrontal cortex. However, the retrograde labeling observed in area TE demonstrates the effectiveness of axonal transport (Fig. 7J).

Two other cases, M5-94 DY and M5-94 FB, had a pattern of labeling that was comparable to case M2-93. Case M5-94 had a rather superficial injection of FB at approximately the same level as case M2-93 (Fig. 2). The pattern and number of labeled neurons were also similar. Labeling was scarce; three labeled neurons in area 10 were found in one section (Fig. 8A). Likewise, a few neurons were present in area 9 (Fig. 8C,F).

Area 46v showed scattered labeled neurons (Fig. 8B). In contrast, area 13 displayed a relatively more abundant amount of labeled neurons, which extended for about 1 mm rostrocaudally, at the border with rostral area 12. Area 13 also had labeling at caudocentral portions of the area, although the labeling was sparse (Fig. 8F). No additional labeling in the caudal part of area 13 was observed. Labeled neurons were predominantly in layer III, although some neurons were at the interface between deep layer VI and the white matter (Fig. 8F).

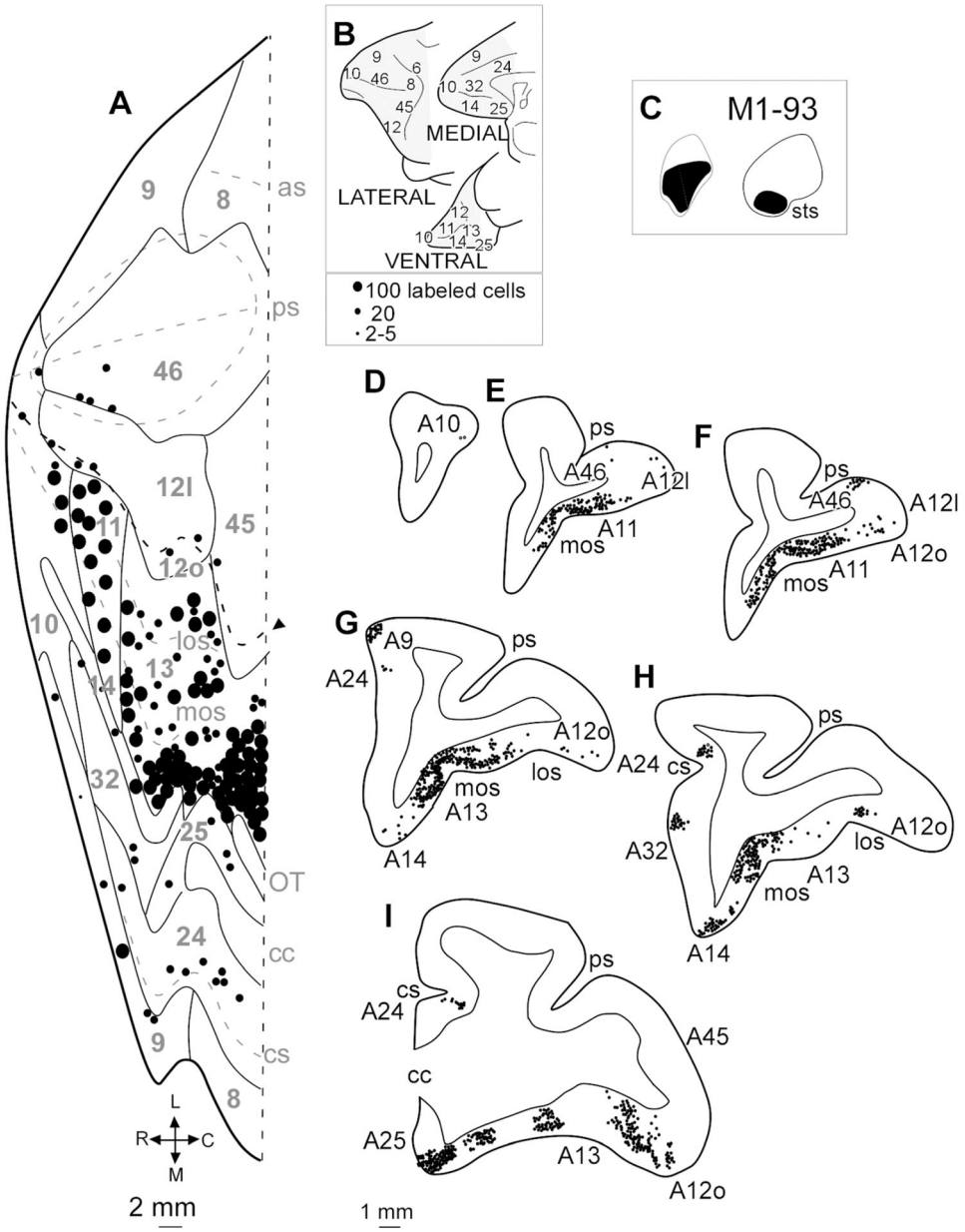

Figure 4. Two-dimensional, unfolded map of the frontal cortex with the representation of retrograde labeled neurons in case M1-93 (**A**), which had the retrograde tracer WGA–HRP deposit in the TPC. Dashed lines indicate the fundus and crown of the frontal sulci and gyri. The arrowheads indicate the lateral border of the frontal lobe that separates area 12l from 12o in this and subsequent figures. **B:** The number of labeled neurons, and frontal cortex areas represented in the unfolded map according to Walker (1940). **C:** Injection site in the ventral part of the TPC in case M1-93. **D–I:** Coronal sectional plots through the frontal lobe from rostral (D) to caudal (I) in which the retrograde labeling observed in this case is presented. Whereas the vLPFC shows a moderate amount of labeled neurons, note the absence of labeling in the dLPFC, in contrast to the dense labeling observed in areas 11 and 13. For abbreviations, see list. Scale bar = 2 mm in A; 1 mm in I (applies to D–I).

Case M5-94 (not shown) had a small DY injection into the medial part of area 36r that resulted in labeling comparable to case M2-93 (Fig. 2), although it was mainly restricted to areas 13 and 14 of the OFC. The vLPFC (area 46v) virtually lacked labeled neurons.

Case M4-94 had a DY injection into the caudal part of area 36r (Fig. 2). Retrograde labeling in area 46v had occasional neurons, at the fundus and ventral bank of the ps (Fig. 8H–K). Area 45 showed a small number of labeled neurons in the midportion of area 45; some of them were also found in layer VI and adjacent white matter (Fig. 8K); retrograde labeling in the lateral part of area 12l decreased caudally (Fig. 8H–J). Label in the OFC was found in areas 12o and 13 of the OFC at

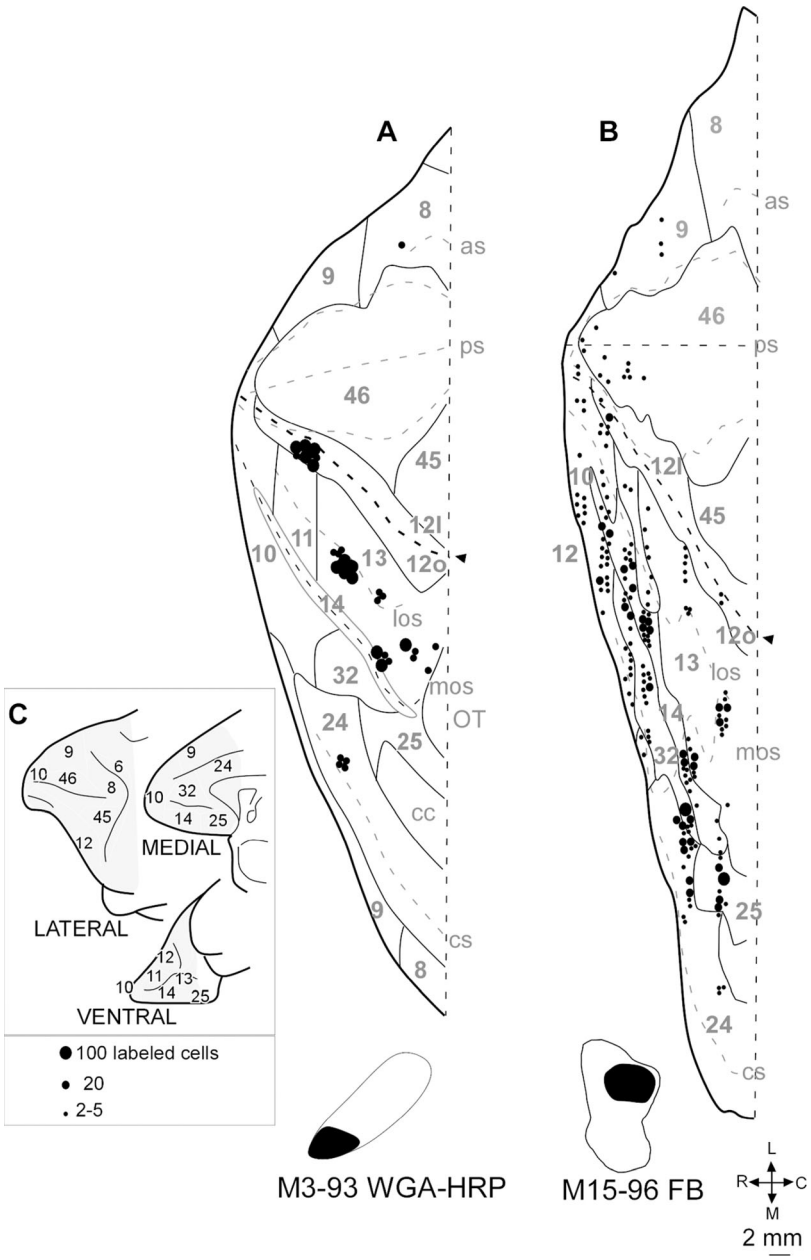

Figure 5. TPC deposits. Two-dimensional representation of the retrograde labeling obtained after tracer deposit in (**A**) the ventral part of the TPC (M3-93, WGA–HRP) and (**B**) the dorsal part of the TPC (M15-96, FB). Conventions are as in Figure 4. For abbreviations, see list. Scale bar = 2 mm in B (applies to A,B).

rostral levels (Fig. 8H–K). The MFC showed a small amount of labeled neurons in areas 24 and 14 (Fig. 8K), whereas area 32 had a slightly higher density of labeled neurons (Fig. 8I,K).

Case M16-96 had a small FB injection into the anterior portion of area 36c at the level of the hippocampal head (Fig. 2), and resulted in lower density of label than in previous cases. Neither the dLPFC nor the vLPFC had retrogradely labeled neurons. Scattered labeled cells were observed in the OFC, some of them in the adjacent white matter, as well as isolated neurons in the MFC (Fig. 9A–E).

In summary, the frontal projection to area 35 was restricted to areas 12o (26%), whereas 12l presented no labeled neurons. Area 13 presented a fair amount of labeled neurons (74%), which, along with area 12o, made up 100% of the OFC labeling. Therefore, only the OFC contributed projections to area 35. Injections in area 36r showed sparse labeling in the vLPFC (45 and 46v, and adjacent area 12l), as well as in the

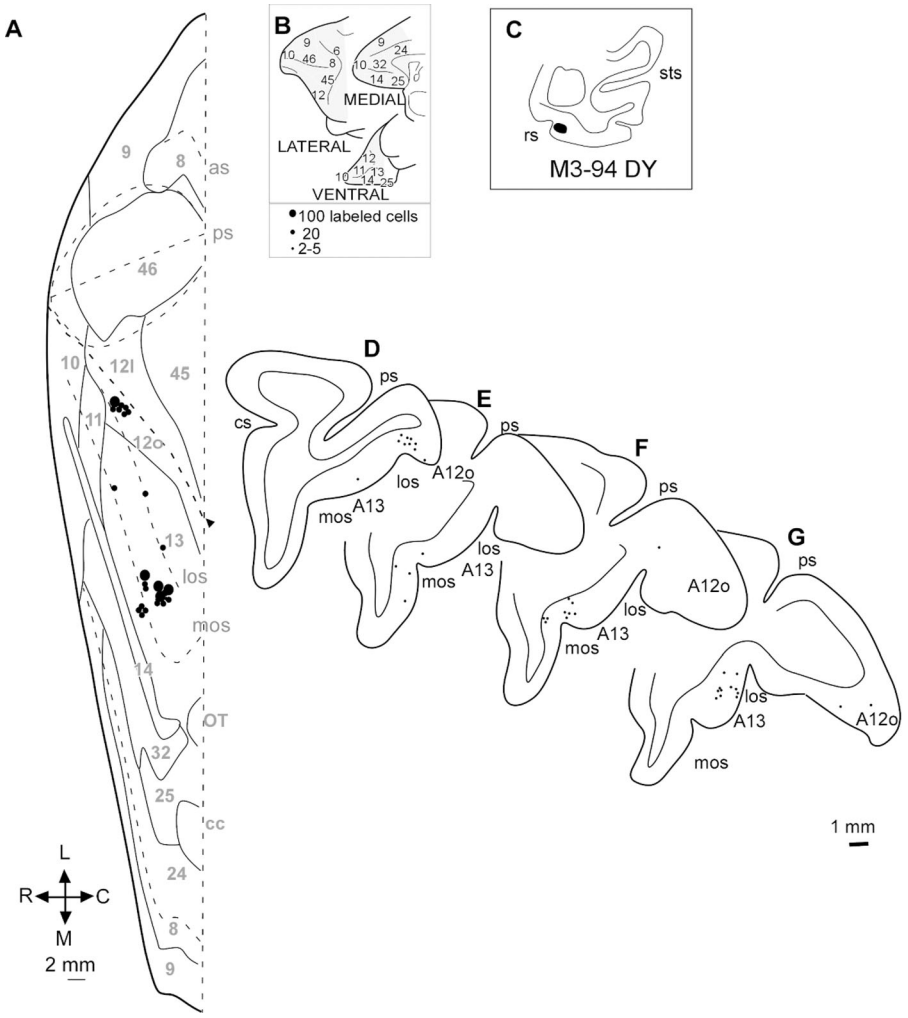

Figure 6. PRC, area 35 deposit. **A:** Two-dimensional unfolded map of case M3-94 DY, which had a deposit in area 35 of the PRC with the representation of neuronal retrograde labeling (dot size equivalence in **B**). **D–G:** Coronal sections through the frontal lobe from rostral (D) to caudal (G) indicate the retrograde labeling found in this case. Note the absence of labeling in the dLPFC and vLPFC. Area 13 also shows low density of labeled neurons. For abbreviations, see list. Scale bar = 2 mm in A; 1 mm in G (applies to D–G).

dorsolateral part of area 9 (three neurons, 0%). Other PFC areas that projected to area 36 were area 10 (18%), area 13 (73%), area 32 (5%), and area 24 (3%). Therefore, these results suggest that very few LPFC afferents were directed to area 36r. In contrast, area 36r was characterized by its connection with area 13 of the OFC. It also received inputs from both the frontal pole (area 10) and the MFC cortex (areas 32).

PFC afferents to inferotemporal cortex based on retrograde tracers

Five cases were included in this group (M6-93 WGA–HRP, M1-96 FB, M15-96 DY, M6-02 FB, and M7-02 FB). The deposit in cases M7-02 FB and M6-02 FB was in the ventral bank of the sts, in area TEa (Fig. 2).

Case M6-93 had a large injection of WGA–HRP in the ventrolateral aspect of the rostral inferior temporal gyrus (area TE1), close to the lateral bank of the anterior middle temporal sulcus (amts), outside the PRC (Figs. 2, 3D). The dLPFC contained no labeled neurons; in contrast, the vLPFC presented labeled neurons that were in continuation rostrally with labeling in the lateral part of the OFC (Figs. 10A–E, 13B). The dorsolateral part of area 12l, at the rostral and midportion of the frontal lobe, showed more than 100 labeled neurons per section, occasionally straddling over the ventralmost portion of area 46v (18%, Fig. 10A,C). The number of labeled neurons at this level decreased for 2–3 mm in the longitudinal axis. An example of retrograde label

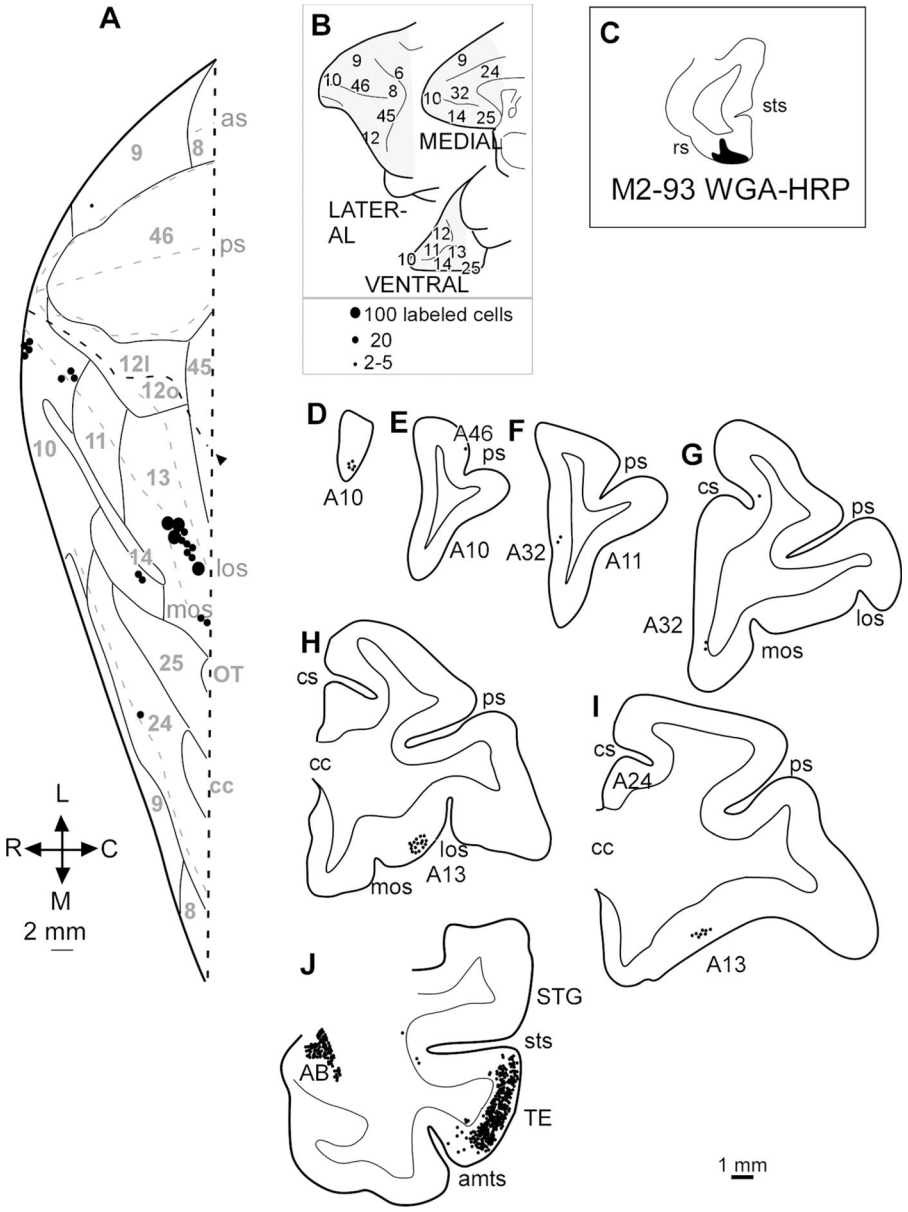

Figure 7. PRC, area 36r deposit. Two-dimensional, unfolded map (**A**) of the frontal cortex with the representation of retrograde labeled neurons in case M2-93 (dot size correspondence with the number of neurons is presented in **B**). **C:** The deposit of WGA–HRP. **D–I:** Coronal sections from rostral (D) to caudal (I) levels. The low density of labeled neurons is noticeable. **J:** More caudal section to show that labeling in the amygdala and area TE indicates that the paucity of labeling in the frontal cortex is not due to a deficient retrograde transport of the label. For abbreviations, see list. Scale bar = 2 mm in A; 1 mm in J (applies to D–J).

in area 12l is shown in Figure 14B. The number of labeled neurons increased up to 300 in the ventrolateral edge of the frontal lobe; up to one-fourth of them were located in the ventralmost portion of area 46v (vLPFC, 6%), and the remainder three-fourths in area 12l (Fig. 10A). This group extended longitudinally for about 4 mm. After a small interval (1–2 mm in a caudal direction) the number of neurons dropped to two to three per section. Labeled neurons continued caudally, as a single patch in rostral area 45 (12%, Fig. 10A,F,G). The number of neurons here was 10–40 per section. A somewhat larger group extended caudally in area 45, as far as the vicinity of the limen insulae.

Abundant retrogradely labeled neurons were found in both OFC areas 11 and 13. Rostrally, the lateral part of area 11 had labeled neurons (1%) that continued into area 12o, which showed 8% of the labeled neurons (Fig. 10A,C,D). Retrograde label in the OFC reached rostral area 13, which had a patch of labeled neurons (up to 100 in a single section [Fig. 10A], accounting for 53%

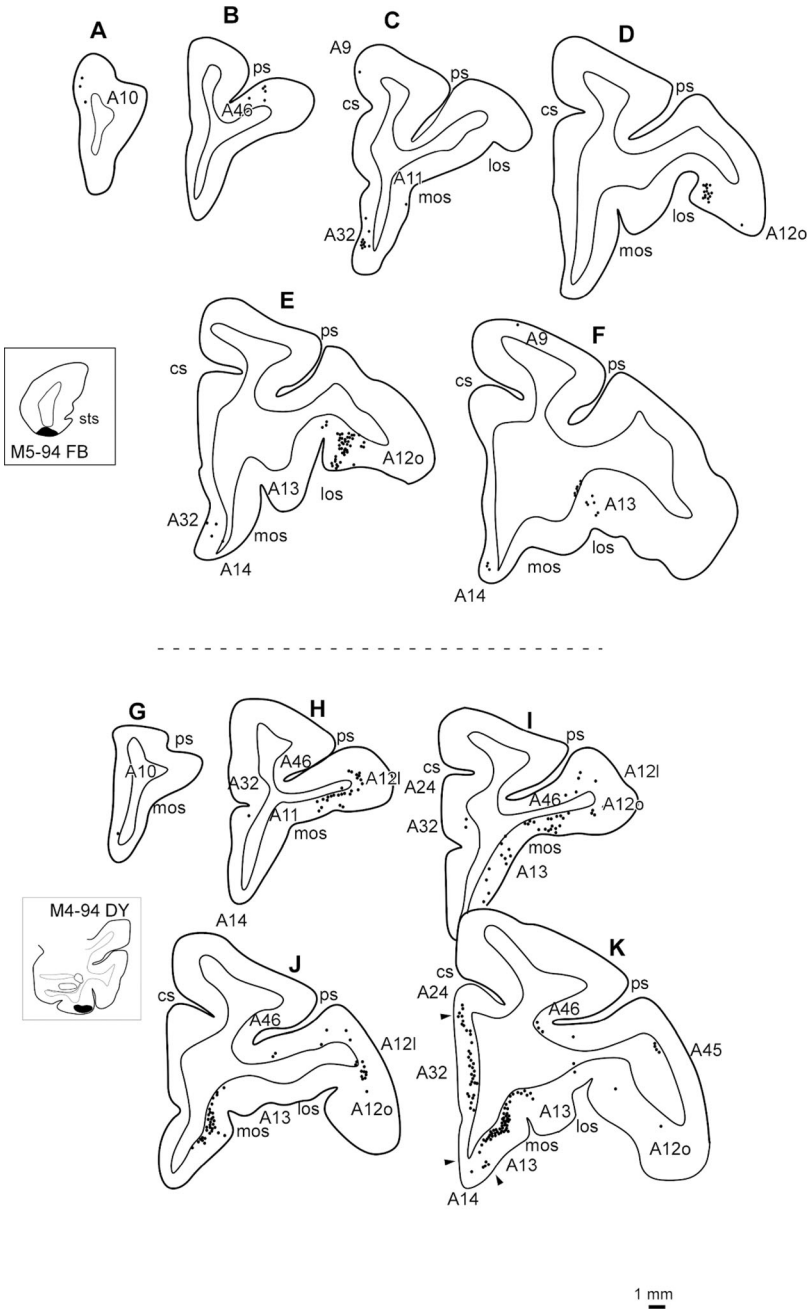

Figure 8. Representation of the distribution of retrogradely labeled neurons after a deposit in rostral area 36r (M5-94, FB, **A–F**) and in caudal 36r area (M4-94, DY, **G–K**). The paucity of retrograde labeling in the vLPFC stands in contrast to the relatively more abundant labeling found after the more caudally placed deposit in M4-94 (**I–K**). Arrowheads point to the boundary between area 32, 24, and 14. Insets show the injection site. For abbreviations, see list. Scale bar = 1 mm in K (applies to A–K).

of the total labeling of 2,400 in the PFC in this case). Labeling was found in layers III and V, between the mos and the los (Figs. 10C–G, 13D, 14A). Retrograde label continued caudally in area 13 as far as the fronto-temporal junction (limen insulae). However, the density of neurons decreased slightly caudal to the level of the genu of the corpus callosum (Fig. 10A). At this point, retrogradely labeled neurons formed two distinct clumps; one was medial, at the level of the mos (up to 170), and, more laterally and caudally, another group had fewer labeled neurons (up to 40), which extended for a total of 5 mm (length) by 1–2 mm (width) as far as the lateral limit of the olfactory tubercle. A small group of labeled neurons continued caudally as far as the agranular insular cortex (not shown). Both layers III and V of the OFC were labeled, but, in contrast to the

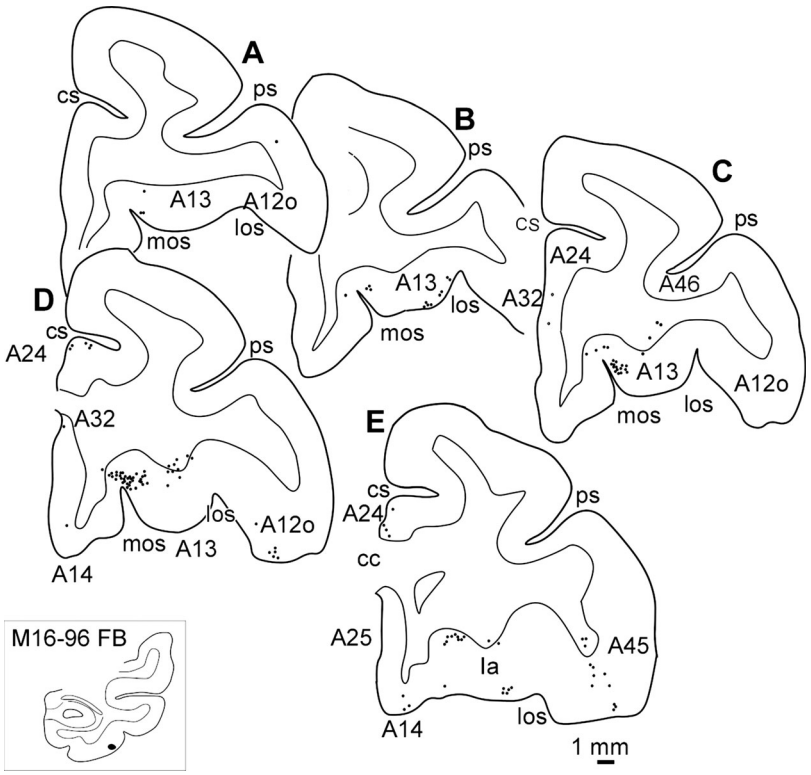

Figure 9. PRC, area 36c deposit. **A–E:** Coronal sections showing the retrograde labeling into the PFC in case M16-96 with a deposit of FB in the lateral part of area 36c (inset). Note the near absence of density of labeled neurons in the dLPFCV as well as the vLPFC. For abbreviations, see list. Scale bar = 1 mm in E (applies to A–E).

previous experiments, a higher density of labeling was present in layer V relative to layer III (Figs. 13D, 14A,B). The MFC was largely devoid of labeled neurons, and only occasional labeled neurons were found in area 24 (1%; Fig. 10A), in area 14 (1%), and in area 25 (1%). Case M1-96 had a small FB injection into the rostral TE1, rostral to previous cases and located at the anterior level of the sts (Fig. 2). Retrograde label was located in two specific regions of the frontal cortex: the vLPFC and OFC (Fig. 10H–J). The vLPFC had a moderate labeling extending from the ventral lip of the ps (area 46v) to the adjacent area 12l (Fig. 10H,I). Further caudally, little labeling was found in the ventral bank of the ps (Fig. 10J). The OFC contained isolated, retrogradely labeled neurons in area 11 (Fig. 10H,I). Caudally, two groups of scattered labeled neurons appeared: a rostral one located at the fundus of the los, and another in between the two orbital sulci, the mos and los, which showed the largest extent and the highest number of neurons. The majority of neurons were in layer III, whereas layer V had fewer labeled neurons. Retrograde labeling decreased caudally.

Case M15-96 had a small DY injection into the rostral TE1, in the transition with area 36r (Fig. 2). The vLPFC had labeled neurons in area 45 (42%), and in the ventral and caudal part of area 46v (16%, the highest value in the series of cases studied) without extending into the dorsal bank of the ps (area 46d). Area 12l presented 1% of labeled neurons. Figure 11A presents the labeling found in this case. A small amount of retrogradely labeled neurons was found in the caudal part of the OFC (areas 12o, 10%, and 13, 32%). In contrast, the MFC was largely devoid of labeled neurons. No retrogradely labeled neurons could be seen in M15-96 (0% in all areas; Fig. 11A). Case M6-93 had 1% in all MFC areas except area 32 (0%).

Case M7-02 had a FB injection in area TEa, near the fundus of the ventral bank of the sts (Fig. 2). Retrograde label was observed in different areas of the frontal lobe (Fig. 12A,D–I). Label was found in the vLPFC (areas 46v, 6%; Fig. 12A,D–H). A small patch of labeled neurons was found in area 45 (2%, Fig. 12A,H,I). Finally, a higher density of labeled neurons was found in area 12l (8%, Fig. 12A,D–H). Isolated neurons were found in the dLPFC (46d, 1%; Fig. 12A,F), as well as in area 9 (0%, nine neurons; Fig. 12A,F). The OFC presented a high density of labeled neurons (areas 11, 27%; 12o, 22%, and 13, 32%). In contrast, the MFC showed only scattered labeled neurons in areas 24 (0%, six neurons) and 32 (0%, six

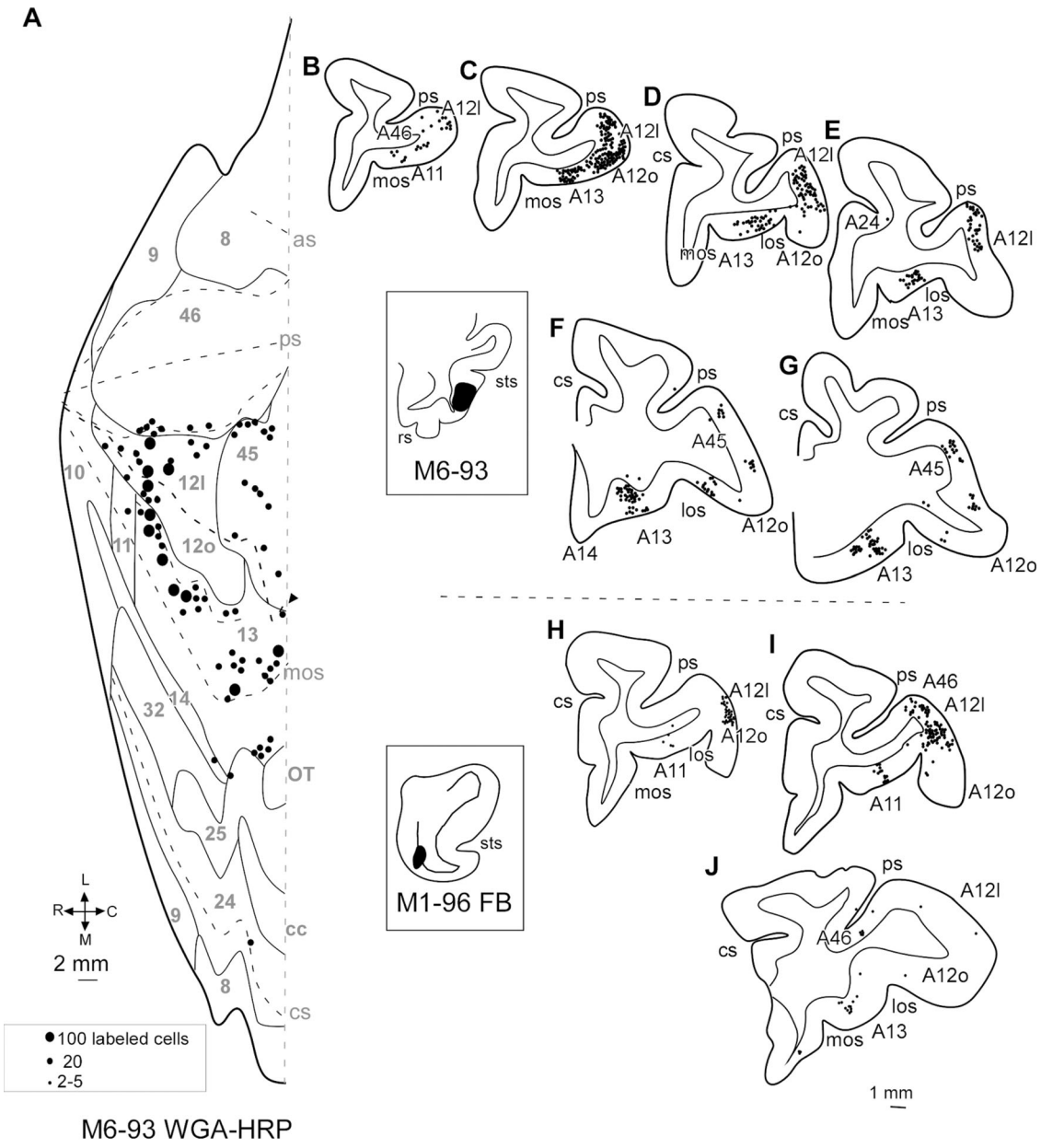

Figure 10. Rostral inferotemporal cortex, area TE. Case M6-93 had a WGA–HRP deposit in the rostral ATL (area TE1, inset). **A:** Two-dimensional, unfolded map of the frontal cortex where retrograde labeled neurons are represented. **B–G:** Representative coronal sections through the frontal lobe with the location of labeled neurons. The higher density of labeling in the vLPFC is noticeable, whereas the dLPFC contains no labeled neurons. **H–J:** Corresponds to a different case (M1-96 FB) with a deposit (inset) at a more rostral level than in case M6-93 shown above. The high density of labeled neurons in the vLPFC can be noticed. Conventions are as in Figure 4. For abbreviations, see list. Scale bar = 2 mm in A; 1 mm in J (applies to D–J).

neurons; Fig. 12A,H). Area 14 had only occasional labeled neurons (0%, six neurons; Fig. 12A,H,I)

Case M6-02 had an FB injection in area TEa of the ventral bank of the sts, caudal to the previous case (Fig. 2). The resulting labeling replicated the pattern of distribution of case M7-02, but the amount of labeled neurons was less. Areas 9 (5%), and 8 (1%; Fig. 11B), contained scattered labeled neurons, but no labeling was observed in area 46d. In addition, substantial labeling in the vLPFC was found at mid and caudal levels of the ventral part of the LPFC (46v, 5%; 45, 12%; and 12l, 13%). The OFC (area 11, 12%; area 12o, 19%; and area 13, 22%) accounted for 44%, whereas the vLPFC accounted for 30%. The MFC presented fewer labeled, neurons than case M7-02 (area 24, 3%; area 14, 7%).

In summary, the results after the tracer deposits in area TE showed that PFC projections originated primarily in the vLPFC (areas 12l, 45, and 46v) and in the

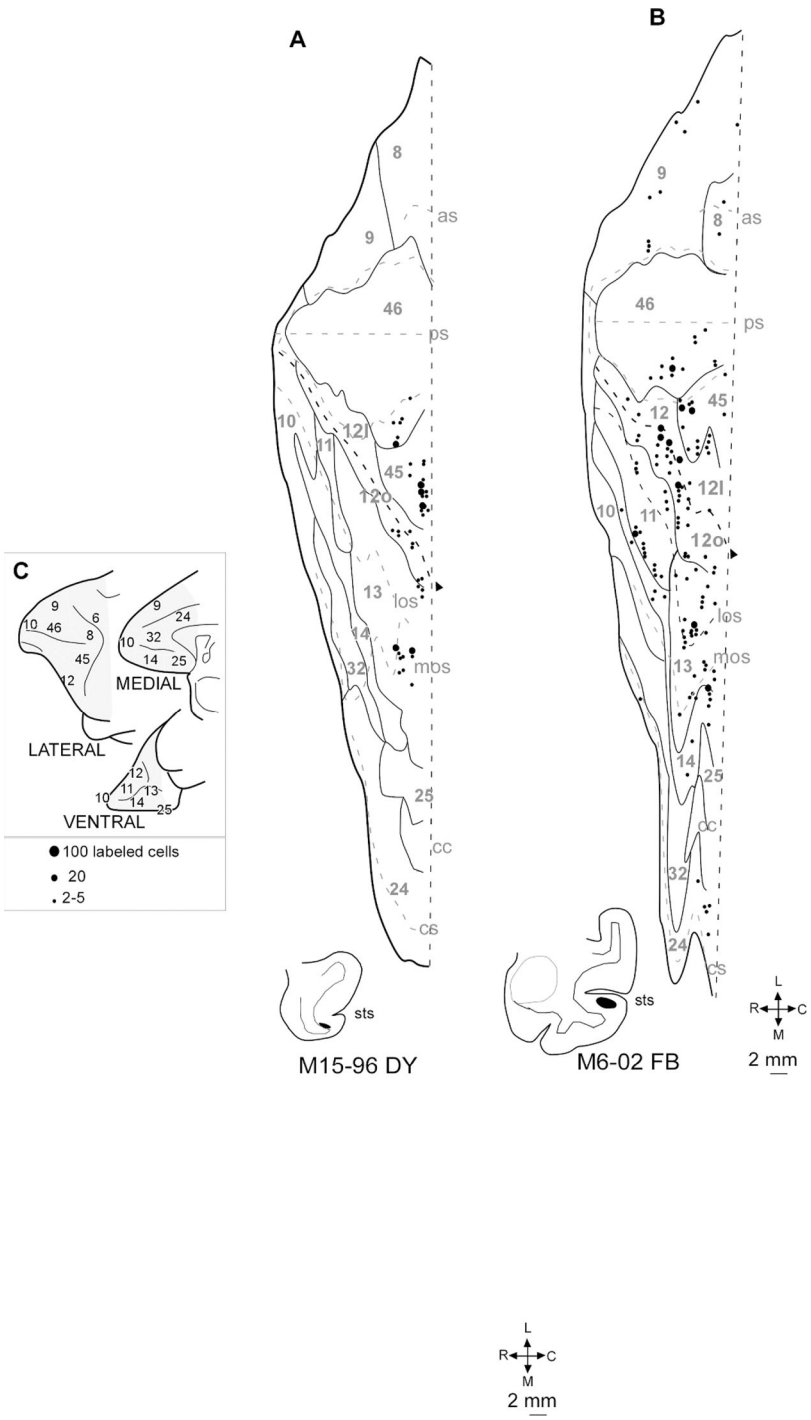

Figure 11. Two-dimensional maps with schematic representation showing retrograde labeling in frontal cortex obtained in cases M15-96 DY (**A**, TE1) and M6-02 FB (**B**, TEa). **C:** The dot size correspondence with the amount of labeled neurons. Conventions are as in Figure 4. For abbreviations, see list. Scale bar = 2 mm in B (applies to A,B).

OFC (areas 11, 12o, and 13). In addition, deposits in area TEa at the ventral bank of the sts showed labeling in the dLPFC, but not after deposits in the TE1. However, vLPFC labeling was roughly similar to TEa deposits. MFC labeling was very light, in both areas 24 and 32, in both cases.

PFC afferents to the posterior parahippocampal cortex based on retrograde tracer injections

Case IM-12 had an FB injection into rostral area TF of the PPH, only for comparative purposes with deposits in the ATL (Fig. 2). Retrograde label was found in

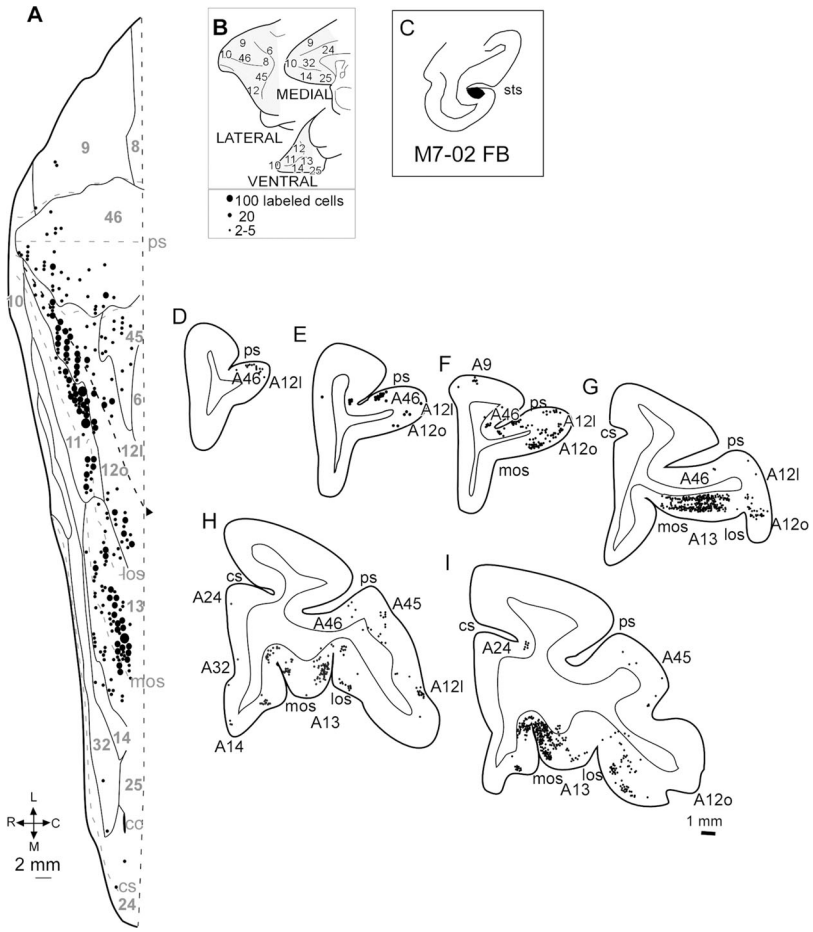

Figure 12. **A–C:** Schematic representation of two-dimensional, unfolded map in case M7-02 FB, which had a deposit in area TEa, placed at a more rostral level than in case M6-02 (Fig. 11B). **D–I:** Distribution of retrograde labeled neurons in a series of coronal sections throughout the frontal cortex. Note the higher density of retrogradely labeled neurons in area 46v relative to other ATL deposits. Conventions are as in Figure 4. For abbreviations, see list. Scale bar = 2 mm in A; 1 mm in I (applies to D–I).

the vLPFC, OFC, and MFC. In the vLPFC, labeled neurons were found in the fundus of the ps (area 46; Fig. 15D,E). Retrograde label in the OFC was primarily located in area 11 (Fig. 15A,B) and in the medial bank of the mos (Fig. 15C). In all these areas, labeled cells were primarily located in layer III. Finally, occasional labeling in the MFC was observed in area 24, but not in area 32 (Fig. 15D,E).

PFC afferents to ATL based on anterograde tracer injections in dLPFC and vLPFC

A total of four cases were included in this group. Two of them had anterograde tracer deposits in the dLPFC, namely, areas 9 (M1-05) and 46d, at the dorsal bank of the ps (M4-05). Two other cases had deposits in the vLPFC, namely, 46v at the ventral bank of the ps (M2-05, M3-05; Table 1, Fig. 2).

In all these experiments except for M4-05, area TEa in the ventral bank and the fundus of the sts had a moderate density of anterograde labeling; likewise, area 35, area 36r of the ATL, and area 36c as well as area TF of the MTL had light density of anterogradely labeled fibers.

Deposits in area 9 of the dLPFC (case M1-05; Fig. 2) resulted in anterogradely labeled fibers in all cortical fields of the ATL, which were continuous with the MTL, although the latter was sparse (Fig. 16). The lateral part of the TPC had a few labeled fibers that continued within the rostral dorsal bank of the sts and other portions of the STG (field STGr of Insausti et al., 1987; Fig. 16B,C). The EL_R subfield of the entorhinal cortex and area 35 of the PRC also contained sparse labeling. However, labeling was virtually absent in area 36r (Fig. 16B,C). The PPH only showed labeled fibers at the caudal portion of area TF.

The area 46d deposit in case M4-05 showed no labeled fibers, either in the TPC or in any other ATL field such as the most anterior part of the superior

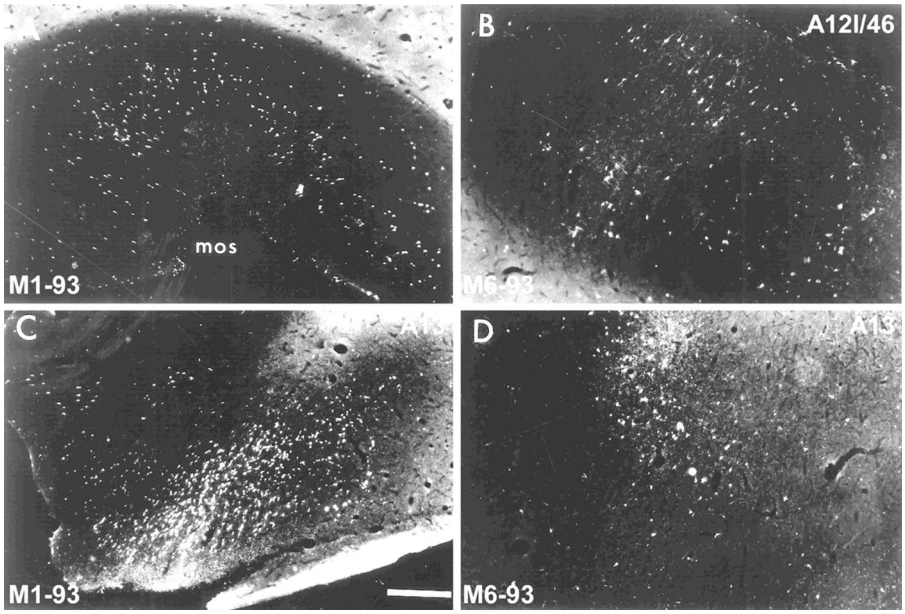

Figure 13. Low-power, darkfield photomicrographs showing neuronal labeling in the OFC (**A, C**) in case M1-93 (temporal polar injection). **B:** Labeling in area 12 and 46v in case M6-93 (rostral area TE injection). **D:** The deep layers of caudal area 13 of the OFC cortex with neuronal labeling after tracer deposit in area TE1. For abbreviations, see list. Scale bar = 500 μm in C (applies to A–D).

temporal gyrus. Anterogradely BDA-labeled fibers in the MTL were also very sparse.

Cases M2-05 (not shown) and M3-05 had an injection in area 46v of the vLPFC (Fig. 2). They showed a different pattern of projection relative to dLPFC deposits. Area 46v projected to the cortex at the fundus of the sts. At the same time, the projection to other areas of the ATL was also sparse (Fig. 16D–F). Only area TEa had labeled fibers (Figs. 16F, 17A).

In summary, area 9 of the dLPFC deposit resulted in very low density of fibers in the ATL, although it covered a larger extent than 46d and 46v deposits. Moreover, area 9 projected more densely to the upper bank of the sts. Area 46d deposits presented no labeled fibers, neither in the ATL (rostral areas 35 and 36) nor in other parts of the MTL (i.e., the entorhinal cortex). In contrast, area 46v presented a moderate projection to the fundus of the sts, and a very light projection to the ATL.

Anterograde tracer injections in the OFC

Two cases had injections in the caudal part of orbital area 13. Case IM-12AA had a ^{3}H-amino acid deposit in the medial part of area 13, and case M6-05 had a BDA injection in area 13 more laterally placed and approximately at the same rostrocaudal level as case IM-12AA (Fig. 2).

Case IM-12 AA has been reported previously (Insausti and Amaral 2008, Fig. 7). The temporal pole showed a high density of anterograde label. In contrast, the remainding areas comprising the ATL showed moderate to light label, limited to the depth and lateral bank of the rhinal sulcus (areas 35 and 36). No label was observed in area TE.

In contrast, deposit in more lateral portions of the OFC (case M6-05) resulted in a high density of anterograde label, in both the ATL and MTL. Overall, most of the labeled fibers were concentrated in the upper bank and fundus of the sts (areas STGf, STGr, and STGi of Insausti et al., 1987; Fig. 16H,I) and in structures of the MTL (i.e., the entorhinal cortex; Figs. 16H,I, 17B). The density of labeled fibers decreased at caudal levels. In addition, a moderate to light density of labeling was found in area TE (Fig. 16H,I).

DISCUSSION

In summary, our results provide evidence that the vLPFC and dLPFC fields present, relative to the OFC and MFC, much weaker or no connectivity with neither the ATL or the MTL. In contrast, the OFC and MFC present strong connectivity. Figure 18 shows a diagram in which our observations are summarized.

LPFC projections to the ATL

Our data suggests a connectional relationship between the LPFC and the ATL that can be summarized as follows: afferents to the ATL from area 46d, plus areas 8 and 9 (the dLPFC), present a different density

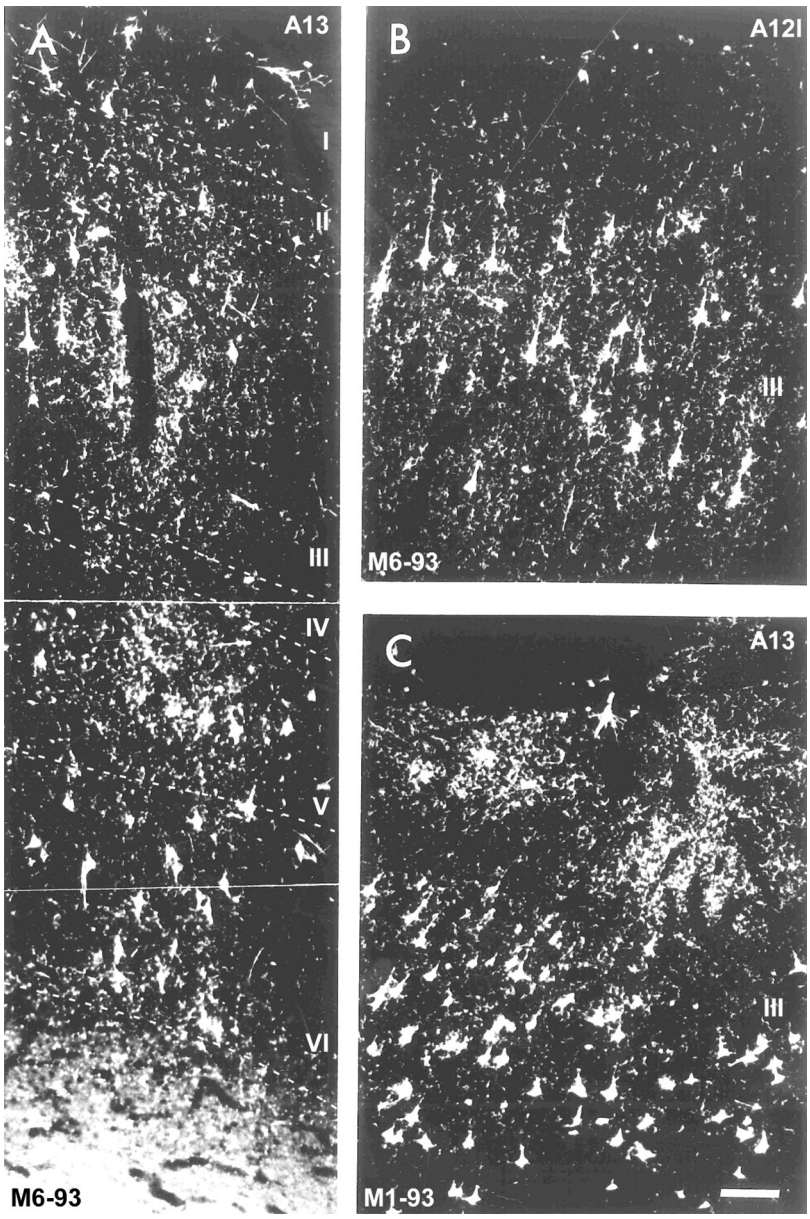

Figure 14. Darkfield photomicrographs of neuron labeling obtained after an injection of WGA–HRP in rostral area TE1 of the inferotemporal cortex (A, B, case M6-93). **A:** Labeling throughout the cortical thickness of area 13 (note the abundant labeling in the deep layers (V–VI). **B:** Retrogradely labeled neurons in layer III of ventrolateral frontal cortex (area 12). **C:** Abundant labeling in layer III of area 13 after a TPC deposit. For abbreviations, see list. Scale bar = 100 μm in C (applies to A–C).

of projections compared with afferents arising in area 46v and areas 12l and 45 (the vLPFC). It should be noted that it is only the rostral portion of the posterior part of the LPFC that originates the input to the ATL, and to a lesser extent, the polar part of the LPFC (Koechlin and Summerfield, 2007).

The dorsalmost part of the dLPFC (areas 9 and 8) resulted in weak projections to the ATL, mostly directed to rostral area TE (TEa), and the dorsal and ventral parts of the TPC; the contribution of area 8 was very small. Overall, the density of labeled neurons in the dLPFC decreased as the deposits were progressively placed more caudally in the ATL, which could indicate a possible posterior boundary of the ATL according to our tracer study.

In contrast, areas 46v, 45, and 12l (the vLPFC) present a distinct and much denser projection to the ATL, although it varied greatly among different areas in the ATL. Whereas the TPC received a weak projection from the vLPFC, the PRC received no projections that could be demonstrated. However, the ATL corresponding to the anterior part of area TE (areas TE1 and TEa of

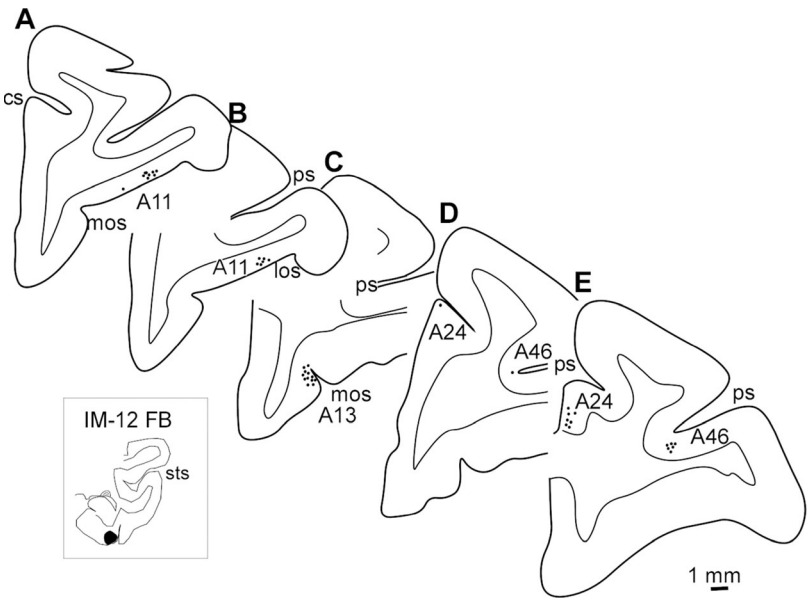

Figure 15. PPH, area TF. **A–E:** Series of coronal sections through the frontal lobe in case IM-12 that had a FB deposit of in area TF of the PPH (inset). Note the scarce amount of retrogradely labeled neurons in the dLPFC. For abbreviations, see list. Scale bar = 1 mm in E (applies to A–E).

Seltzer and Pandya, 1978) of the inferotemporal cortex received moderate to dense projections from the vLPFC; Ban et al. (1991) observed that after HRP injections in the Tea, some labeling was observed in area 46v/45. By comparison, frontal cortex afferents to the PPH were also limited (Suzuki and Amaral, 1994a). The rostralmost part of the STG cortex that we have included as part of the ATL showed a different pattern of labeling relative to other ATL regions. The dLPFC (experiment M1-05) had a sparse projection to the dorsal bank of the sts. The vLPFC presented moderate labeling at the ventral bank (extending into the fundus) of the sts (case M3-05). Previous reports also noted that the rostral STG is connected mainly with the vLPFC, as shown by both anterograde (Gerbella et al., 2010, case 37r; Gerbella et al., 2013, case 51r) and retrograde labeling (Barbas and Mesulam, 1981, area 8; Markowitsch et al., 1985, areas 46v and 46d). In contrast, the OFC (case M6-05) displayed strong labeling in both banks of the sts.

The results obtained in this experimental series are in agreement with a more extensive analysis of the afferents to the PPH reported by Suzuki and Amaral (1994a, their Fig. 13). In that report, several retrograde tracer deposits were placed at different rostrocaudal and mediolateral locations of the TF-TH, and the resulting labeling in the dLPFC was moderate or low. In addition, their deposits were located more caudally than ours (M-2-90). In the same report, afferents to the PRC were also studied, and our findings are consistent and extend those obtained by Suzuki and Amaral (1994a). Our retrograde tracer deposits were focused on the rostral part of areas 35 and 36, and support the paucity of projections of the dLPFC to the PRC located in the ATL. Other studies also provide partial information on the issue of LPFC projections to areas in the ATL. Among them are the classic retrograde tracer studies of Markowitsch et al. (1985), Moran et al. (1987), and Kondo et al. (2003). These reports show deposits at different ATL locations, and we will discuss our results specifically compared with each one. Markowitsch et al. (1985) present mainly temporal pole deposits, although these encroached on other ATL areas as well (i.e., case R3). Our results are consistent with the pattern of labeling in the PFC area 10 after TPC deposits. Deposits that extended to rostral area TE (cases R2 and R3) resulted in the highest number of labeled neurons in the vLPFC (46v and 12l). Interestingly, no labeled neurons were found in the dLPFC. Moran et al. (1987) showed retrograde tracer deposits restricted to the TPC. Our results confirm the pattern of projections after our TPC deposits, in particular the near absence of labeling in the dLPFC and the limited amount in the vLPFC. Only area 10 seemed to contain consistently retrogradely labeled neurons. The more recent study of Kondo et al. (2003) presents the results after limited tracer deposits in the temporal pole, with which our results are in agreement. In contrast to the reports of Markovitsch et al. (1985) and Moran et al. (1987), our labeling in areas 9 and 8 replicates the findings of

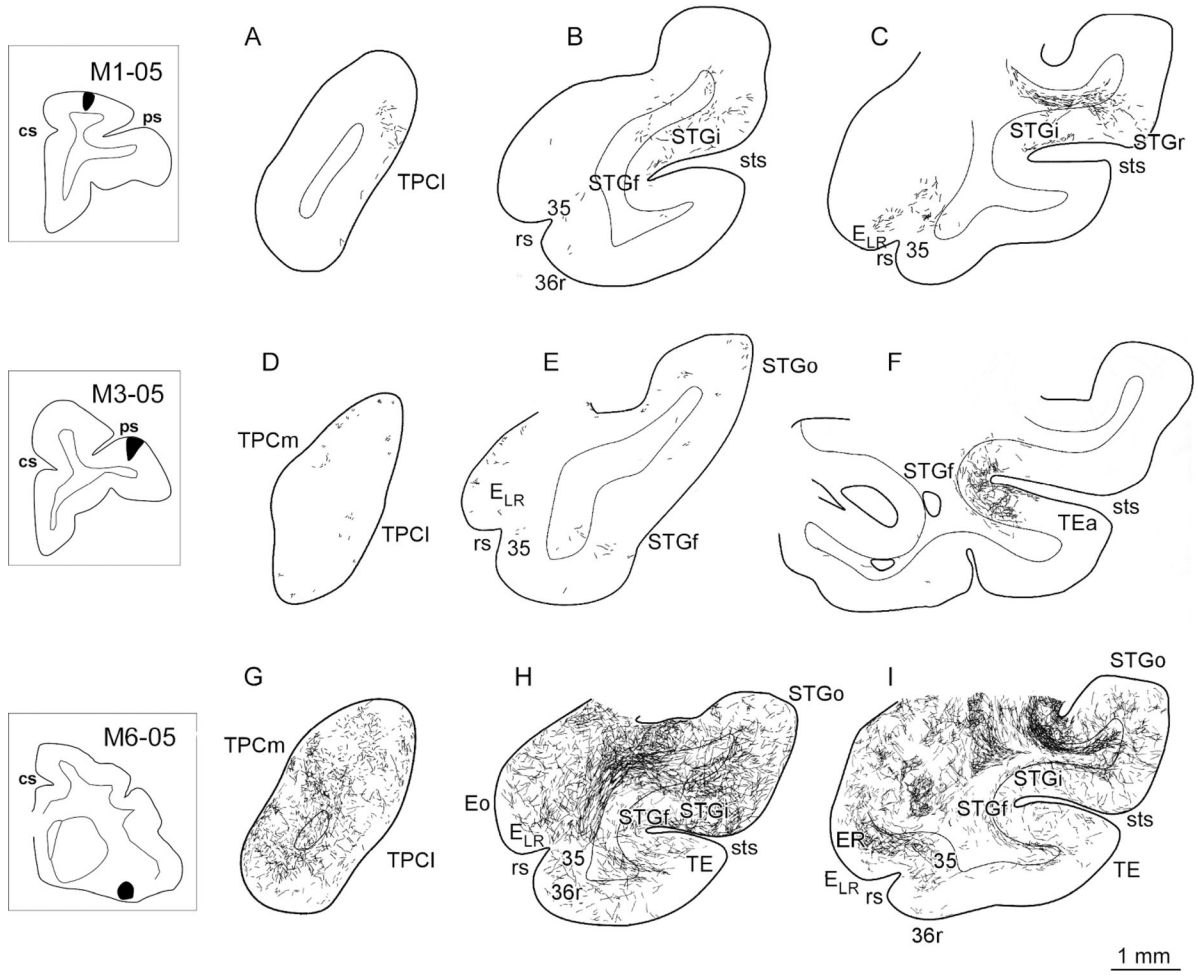

Figure 16. PFC, Schematic representation of ATL labeling obtained after deposits of anterograde tracer into the dLPFC, vLPFC, and OFC as seen in coronal sections. **A–C:** Anterograde labeling in the ATL after dLPFC (area 9) deposit (case M1-05). **D–F:** Anterogradely labeled fibers after a deposit in area 46v (case M3-05). **G–I:** Labeled fibers after OFC deposit in area 13 (case M6-05). For abbreviations, see list. Scale bar = 1 mm in I (applies to A–I).

Kondo et al. (2003). These three studies are representative of the findings reported in the literature, and all coincide in showing a paucity of LPFC afferents to the ATL. Our present results support this contention.

The scarce projection is restricted to the vLPFC (areas 46v and 12l), contrasting with the almost complete absence of retrograde labeling in the dLPFC (area 46d), whereas sparse connectivity was found in areas 9 and 8. In addition, the previously cited reports, as well as our results, are in agreement in terms of the heavy connectivity with the OFC and MFC (see below). This fact indicates that no technical pitfall in the use of these retrograde tracers in our study would account for the sparse (vLPFC) or almost total absence (dLPFC) of connections with the ATL.

Conversely, the scarcity or absence of LPFC afferents to the ATL is further supported by our anterograde transport data. The BDA and ^{3}H amino acid labeling in the ATL shows a gradation in the density of anterogradely labeled fibers: areas 9 and 46 showed weak or no projections to the ATL, whereas deposits in area 46v resulted in a moderate-to-light projection. In contrast, deposits in the OFC (medial and lateral area 13) showed a heavy projection to the ATL. Those findings extend previous work with tracing techniques. The classical studies in the monkey made by Jones and Powell (1970), and Van Hoesen et al. (1975), by ablating various parts of the frontal cortex, showed that the whole ATL receives afferents from the frontal cortex, but the methodology used made it impossible to determine the exact origin of these projections. Jones and Powell (1970) show that lesions in area 9 result in light density of degeneration in the ATL (cases OM 78 and 69). Pandya et al. (1971) extend these findings with lesions in the upper bank of the ps, but they do not show degenerating fibers in the ATL. In contrast, the lesion in the

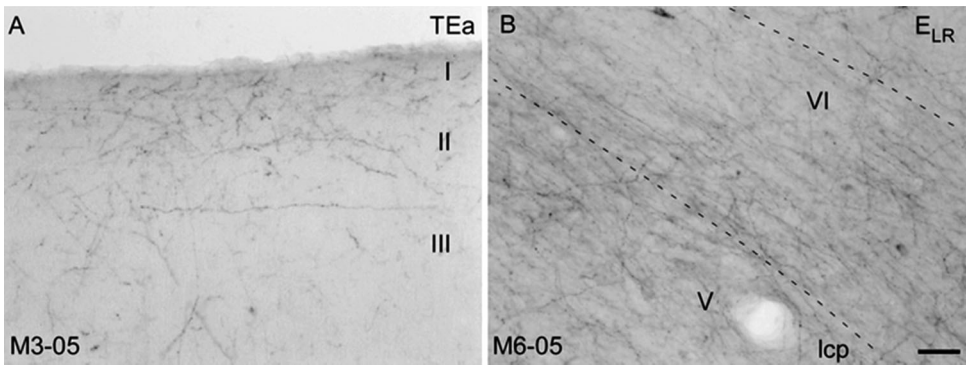

Figure 17. **A:** Photomicrographs of BDA-labeled fibers in area TEa after a BDA deposit in the ventral bank of area 46 (vLPFC) in case M3-05. **B:** Labeling in area 35 and adjacent entorhinal cortex subfield E_{LR} after a BDA deposit in the lateral part of area 13 of the OFC (case M6-05). Note the moderate density of the anterograde labeling in area TEa. In contrast, the density of BDA-labeled fibers is higher after the OFC injection. For abbreviations, see list. Scale bar = 100 μm in B (applies to A,B).

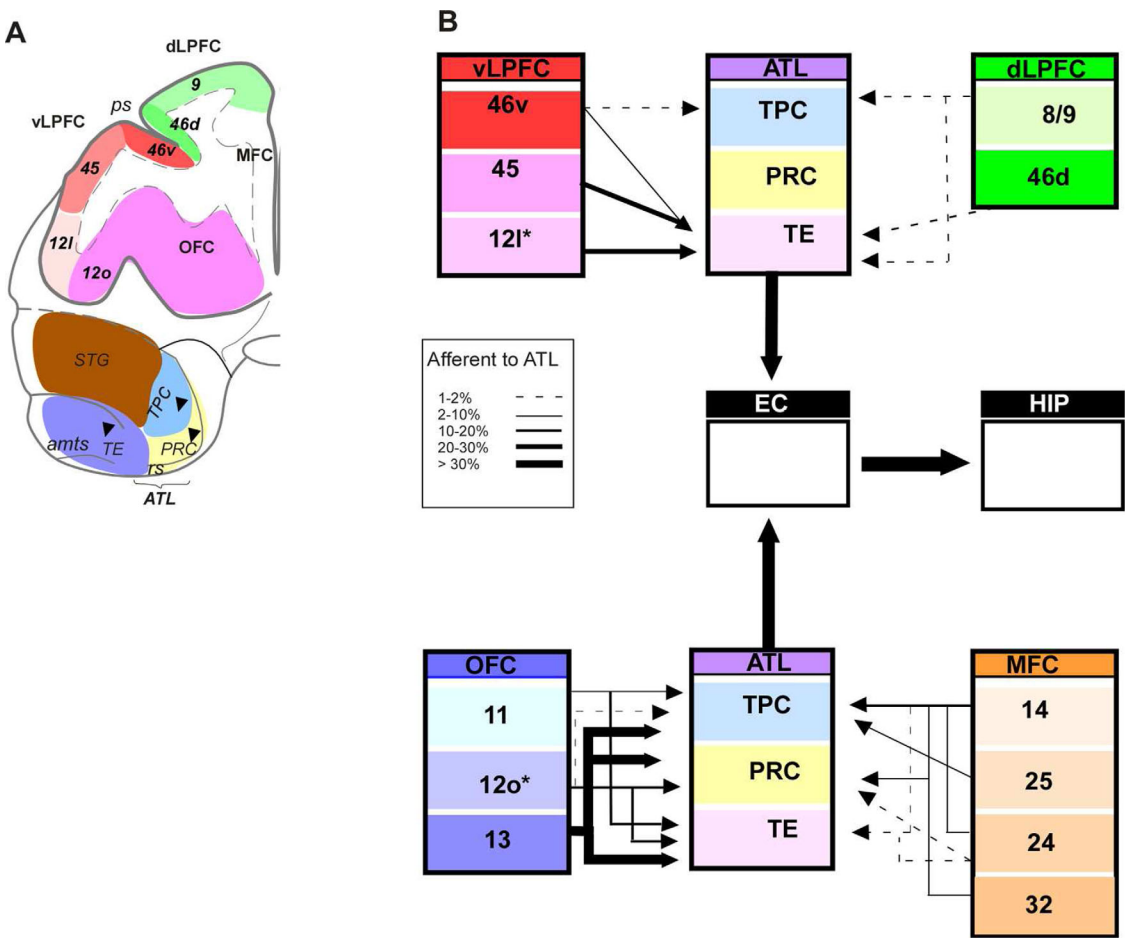

Figure 18. Summary diagram of the topography of the areas (**A**) and connectivity between the ATL and the LPFC (**B**). In the upper part of B, the projection form the LPFC to the ATL is represented. The lower part shows the projections from the OFC and MFC to the ATL. The thickness of the arrow is scaled to the percentage shown in Table 2B, corresponding to the density of the projection to the ATL. Dashed line means low density of projection. For abbreviations, see list.

ventral bank of the ps (case 11) or area 10 (case 1) showed degeneration at places compatible with the ATL (Pandya et al., 1971, Figs. 1, 2).

The laminar origin of this projection further supports the difference between area TE in the ATL and the remainder (rostral PRC and TPC). Whereas rostral inferotemporal cortex injections labeled both layers III and V, TPC and PRC injections preferentially labeled layer III of areas of the vLPFC. Although the laminar origin of the PFC projection based on the retrograde labeling experiments in our study suggests a feed-forward pattern according to the criteria of Felleman and van Essen, (1991), a more complex PFC pattern of lamination than in other cortical regions, depending on the cortical organization of the specific areas under study, has been reported (Rempel-Clower and Barbas, 2000).

In addition, it is worth noting that overall the frontal cortex afferent projection to the ATL is moderate, at most. Data in the literature extend this pattern to the whole PHR. This contention is supported by the findings of Suzuki and Amaral (1994a), because little or no frontal cortex projection to areas 36c of the PRC and TF-TH of the PPH is described. Although we did not inject the rostralmost portion of the STG, there are data in the literature that support our argument (Pandya and Kuypers, 1969; Seltzer and Pandya, 1978).

Orbitofrontal cortex projections to the ATL

The injected retrograde and anterograde tracers demonstrated that the OFC projects to all components of ATL. Overall, the projections from the OFC to the ATL were by and large the most abundant, although several distinct patterns could be observed in our study. Area 13 of the OFC was the only cortical region that projected to all components of the ATL. Area 11 also projected to most of the fields, excluding the PRC. The TPC received a strong projection from the midportion of area 11 that reached as far as the boundary with area 13. The rostral PRC (areas 35 and 36) receives a lighter projection from mid- or medial portions of caudal area 13. The only case in our series with an injection in the PPH, by comparison, showed a pattern of labeling similar to that of the rostral PRC. Rostral area TE of the inferotemporal cortex also seemed to receive a heavy projection from the OFC, whose density was in between the projection to the TPC and the PRC. This projection originated in most of the extent of area 13 located between the medial and lateral orbital sulci. Additional labeling was found in area 10, but it was restricted to a few individual neurons at the rostral tip of the frontal cortex. Interestingly, this projection was only found after area 36 tracer deposits. This finding is in agreement with the results of Medalla and Barbas (2014) and Kondo et al. (2005, Fig. 4C), which complement the results described by Suzuki and Amaral (1994a).

A hint of topography could be detected in our data with OFC labeling from the ATL. Columns of labeled neurons in area 13 were arranged from medial (TPC), intermediate (rostral PRC), and lateral (extending into areas 12l and 45), to rostral area TE. The strip of cortex that borders the olfactory tract and tubercle laterally (area Pall of Barbas and Pandya, 1989; Barbas, 1993; area Iapm-Iam of Carmichael and Price, 1994) had in particular a dense concentration of labeled neurons. Our results confirm experimental work performed in macaque monkeys injected with retrograde tracers into the TPC showing labeling in the OFC (Markowitsch et al., 1985; Moran et al., 1987; Shiwa, 1987; Seltzer and Pandya, 1989).

The OFC projection to the rostral PRC deserves particular attention as it is rather light compared with the robustness of other cortical inputs (Martin-Elkins and Horel, 1992; Suzuki and Amaral, 1994a). Suzuki and Amaral (1994a) show denser PFC afferent projections to the PRC than our observations. However, many of their retrograde tracer deposits were placed at more caudal levels, possibly outside the ATL; moreover, the most rostral injection case (M-21-91) also shows weaker frontal cortex labeling, similar to our results. Our findings not only confirm the above studies, but also add further support for the idea that OFC projections to the rostral PRC are less extensive, because they are mainly restricted to dense, but quite confined patches of labeling. Despite the high percentage of labeling in the OFC (73%) the total number of labeled neurons was the lowest of all labeling in the ATL.

Medial prefrontal cortex projections to the ATL

Injections involving the TPC at the dorsal portion of the ATL yielded substantial labeling in the MFC, specifically in the portion that lies under the corpus callosum, infralimbic cortex (area 25), although labeling at more rostral MFC areas (rostral areas 24 and 32) confirms previous studies (Moran et al., 1987, case A; Shiwa, 1987, case Com 73; Barbas et al., 1999; Carmichael and Price, 1995; Kondo et al., 2003). These studies and ours suggest that infralimbic afferents to cortex of the ATL are directed preferentially to the dorsal part of the TPC. Rostral PRC and anterior area TE deposits virtually lacked labeling in the MFC other than a few scattered neurons, mainly in the rostralmost portion of areas 24 and 32 (rostral PRC), and 14 and 24 (rostral area TE) after retrograde tracer injections. Similar results were described by Suzuki and Amaral (1994a), although

Kondo et al. (2005) reported a light projection to the ATL from the caudalmost part of area 25. Suzuki and Amaral (1994a) extend those results to the PPH, as they do not report MFC labeling from more caudal portions of the TF. Therefore, it can be concluded that the ATL component that receives projections from the MFC is the dorsal part of the TPC, in particular from the infralimbic cortex, and less so from the anterior cingulate cortex.

Frontal–ATL interactions: functional implications

Ablation studies of the vLPFC cause perseverative interference in monkeys, but preserve visual pattern discrimination, a function that depends largely on area TE of the inferotemporal cortex (Iversen and Mishkin, 1970). These findings suggest that vLPFC connections with the temporal cortex are not necessary to sustain visual recognition per se, but rather to provide a temporal structure to behavior. Similar lesions have been reported to produce deficits in delayed matching to colors (Passingham, 1975), although further studies (Kowalska et al., 1991) reported no effect on recognition memory tests (delayed nonmatching-to-sample). However, the removal of the OFC and MFC impairs visual recognition memory on delayed nonmatching-to-sample tasks as well as hyperorality (Bachevalier and Mishkin, 1986).

Taking into consideration the visual responses found in the vLPFC, it is likely that the rostral TE cortex participates, in conjunction with the frontal eye fields, in the integration of visually guided motor response (Kubota and Suzuki, 1973; Mikami et al., 1982; Suzuki and Anuma, 1983; Boch and Goldberg, 1989). The analysis of form, which largely depends on the inferotemporal cortex (Baylis et al., 1987; Miyashita et al., 1993; Horel, 1994), could receive information on the elaboration of oculomotor responses (Ringo et al., 1994).

Afferent projections from polysensory (Kawamura and Naito, 1984; Barbas, 1988; Petrides and Pandya, 1988) and olfactory areas (Carmichael et al., 1994), as well as intrinsic (OFC and MFC) afferents to the vLPFC, orbital, and medial frontal cortices (Pandya and Yeterian, 1990; Morecraft et al., 1992) would allow the flow of this highly elaborated information to the ATL, and ultimately to the entorhinal cortex (Insausti et al., 1987; Suzuki and Amaral, 1994b; Insausti and Amaral, 2008). Here, information could be relayed directly to the hippocampus. In contrast, the anterior area TE of the inferotemporal cortex directly projects to a very small part of the entorhinal cortex (Saleem and Tanaka, 1996; Mohedano-Moriano et al., 2007), and therefore, has limited direct access to the caudal hippocampus. Its main entry is via the PRC (Insausti et al., 1987; Suzuki and Amaral, 1994b), although the relative importance of each of these pathways is unknown.

The functional implication of such a specific pattern of projections from the frontal cortex to the ATL is worth considering. One approach is to explore the consequences of the disconnection between the frontal and the temporal lobes by sectioning the uncinate fascicle, which is the main pathway that connects the OFC with the ATL (Ungerleider, 1989; Gloor, 1997). The experimental frontotemporal disconnection by section of the uncinate fascicle impairs visuomotor and visual–visual associative learning while leaving intact performance in the delayed-matching to sample (DNMS) task (Gaffan and Eacott, 1995). Spared memory performance in the DNMS after the uncinate fascicle lesion could perhaps be because this lesion leaves intact the ATL cortex (Eacott and Gaffan, 1992), as well as many of the nonfrontal cortex connections of the temporal lobe, including those with the amygdala (Ungerleider et al., 1989) and diencephalon. Because our study shows that the rostral part of the PRC is only sparsely connected with the PFC, it is likely that such behavioral deficits are primarily due to the disconnection between rostral area TE and the PFC. It seems less likely that the impairment could be attributed to the disconnection of the TPC and PFC, as this lesion usually produces Klüver–Bucy syndrome (Klüver and Bucy, 1939; Myers, 1972; Eacott and Gaffan, 1992), a deficit not reported in the afore mentioned study.

In conclusion, our results, taken together with previous anatomical and functional studies, suggest that polysensory information related to functional activity of the frontal lobe (and possibly also to working memory) is barely conveyed to the ATL through the dLPFC, and very little is conveyed through the vLPFC to the MTL (Koechlin and Summerfield, 2007; Fuster, 2008). In contrast, a direct influence is made possible by stronger relationships with the OFC and to a lesser extent with the MFC (Barbas et al., 1999). Indirectly, however, and through intrinsic connections of the frontal lobe (Barbas and Pandya, 1989; Carmichael and Price, 1995; Petrides et al., 2012), the dLPFC and vLPFC could reach the ATL, and along with the remainder of the PHR may access the entorhinal cortex and the hippocampus formation (Insausti et al., 1987; Insausti and Amaral, 2012).

ACKNOWLEDGMENTS

We acknowledge the technical help of Purificacion Botín, Carmentxu García Gortari, Mercedes Íñiguez de Onzoño, Guillermo Lozano, Carmen Ruiz, Isabel Úbeda,

Isidro Medina, and María Luisa Ramos-Herrera. We also thank the personnel of the animal quarters at the Universities of Navarra and Castilla-la Mancha. We also express our gratitude to Dr. David G. Amaral (University of California, Davis and the MIND Institute) for providing us with some of the material

CONFLICT OF INTEREST STATEMENT

The authors declare that they have no identified conflicts of interest.

ROLE OF AUTHORS

All authors take responsibility for the integrity of the data and the accuracy of the data analysis. Study concept and design: RI. Experimental procedures and acquisition of data: EAS, AMI, MML, Alicia MM, PPS, Alino MM, EAP, MMA, MPM, SCC, ELG, RI. Analysis and interpretation of data: EAS, MML, PPS, Alicia MM, RI. Drafting of the manuscript: RI. Critical revision of the manuscript for important intellectual content: RI, Alicia AMM, MML. Technical and material support: EAS, AMI, MML, Alicia MM, PPS, Alino MM, EAP, MMA, MPM, SCC, RI. Study supervision: RI.

LITERATURE CITED

Amaral DG, Insausti R, Cowan WM. 1987. The entorhinal cortex of the monkey: I. Cytoarchitectonic organization. J Comp Neurol 264:326–355.

Arikuni T, Sako H, Murata A. 1994. Ipsilateral connections of the anterior cingulate cortex with the frontal and medial temporal cortices in the macaque monkey. Neurosci Res 21:19–39.

Bachevalier J, Mishkin M. 1986. Visual recognition impairment follows ventromedial but not dorsolateral prefrontal lesions in monkeys. Behav Brain Res 20:249–261.

Ban T, Shiwa T, Kawamura K. 1991. Cortico-cortical projections from the prefrontal cortex to the superior temporal sulcal area (STs) in the monkey studied by means of HRP method. Arch Ital Biol 129:259–272.

Barbas H. 1988. Anatomic organization of basoventral and mediodorsal visual recipient prefrontal regions in the rhesus monkey. J Comp Neurol 276:313–342.

Barbas H. 1993. Organization of cortical afferent input to orbitofrontal areas in the rhesus monkey. Neuroscience 56: 841–864.

Barbas H, Pandya DN. 1989. Architecture and intrinsic connections of the prefrontal cortex in the rhesus monkey. J Comp Neurol 286:353–375.

Barbas H, Ghashghaei H, Dombrowski SM, Rempel-Clower NL. 1999. Medial prefrontal cortices are unified by common connections with superior temporal cortices and distinguished by input from memory-related areas in the rhesus monkey. J Comp Neurol 410:343–367.

Baylis GC, Rolls ET, Leonard CM. 1987. Functional subdivisions of the temporal lobe neocortex. J Neurosci 7:330–342.

Benevento LA, Fallon J, Davis BJ, Rezak M. 1977. Auditory–visual interaction in single cells in the cortex of the superior temporal sulcus and the orbital frontal cortex of the macaque monkey. Exp Neurol 57:849–872.

Binney RJ, Embleton KV, Jefferies E, Parker GJ, Ralph MA. 2010. The ventral and inferolateral aspects of the anterior temporal lobe are crucial in semantic memory: evidence from a novel direct comparison of distortion-corrected fMRI, rTMS, and semantic dementia. Cereb Cortex 20:2728–2738.

Boch RA, Goldberg ME. 1989. Participation of prefrontal neurons in the preparation of visually guided eye movements in the rhesus monkey. J Neurophysiol 61:1064–1084.

Bonnici HM, Chadwick MJ, Lutti A, Hassabis D, Weiskopf N, Maguire EA. 2012. Detecting representations of recent and remote autobiographical memories in vmPFC and hippocampus. J Neurosci 32:16982–16991.

Borra E, Gerbella M, Rozzi S, Luppino G. 2011. Anatomical evidence for the involvement of the macaque ventrolateral prefrontal area 12r in controlling goal-directed actions. J Neurosci 31:12351–12363.

Brodmann K. 1909. Vergleichende Lokalisationslehere der Grosshimrinde in ihren Principien dargestellt auf des Grund des Zellenbayes. Leipzig, Germany: Barth.

Brown MW, Wilson FA, Riches IP. 1987. Neuronal evidence that inferomedial temporal cortex is more important than hippocampus in certain processes underlying recognition memory. Brain Res 409:158–162.

Bruce C, Desimone R, Gross CG. 1981. Visual properties of neurons in a polysensory area in superior temporal sulcus of the macaque. J Neurophysiol 46:369–384.

Carmichael ST, Price JL. 1994. Architectonic subdivision of the orbital and medial prefrontal cortex in the macaque monkey. J Comp Neurol 346:366–402.

Carmichael ST, Price JL. 1995. Limbic connections of the orbital and medial prefrontal cortex in macaque monkeys. J Comp Neurol 363:615–641.

Carmichael ST, Clugnet MC, Price JL. 1994. Central olfactory connections in the macaque monkey. J Comp Neurol 346:403–434.

Cavada C, Goldman-Rakic PS. 1989. Posterior parietal cortex in rhesus monkey: II. Evidence for segregated corticocortical networks linking sensory and limbic areas with the frontal lobe. J Comp Neurol 287:422–445.

Cavada C, Company T, Tejedor J, Cruz-Rizzolo RJ, Reinoso-Suarez F. 2000. The anatomical connections of the macaque monkey orbitofrontal cortex. A review. Cereb Cortex 10:220–242.

Corbetta M, Akbudak E, Conturo TE, Snyder AZ, Ollinger JM, Drury HA, Linenweber MR, Petersen SE, Raichle ME, Van Essen DC, Shulman GL. 1998. A common network of functional areas for attention and eye movements. Neuron 21:761–773.

Cowan WM, Gottlieb DI, Hendrickson AE, Price JL, Woolsey TA. 1972. The autoradiographic demonstration of axonal connections in the central nervous system. Brain Res 37:21–51.

Curran E.J. 1909. A new association fiber tract in the cerebrum (with remarks on the fiber tract dissection method of studying the brain). J Comp Neurol 19:645–657.

Desimone R, Gross CG. 1979. Visual areas in the temporal cortex of the macaque. Brain Res 178:363–380.

Distler C, Boussaoud D, Desimone R, Ungerleider LG. 1993. Cortical connections of inferior temporal area TEO in macaque monkeys. J Comp Neurol 334:125–150.

Eacott MJ, Gaffan D. 1992. Inferotemporal-frontal disconnection: the uncinate fascicle and visual associative learning in monkeys. Eur J Neurosci 4:1320–1332.

Fahy FL, Riches IP, Brown MW. 1993. Neuronal activity related to visual recognition memory: long-term memory and the encoding of recency and familiarity information in the primate anterior and medial inferior temporal and rhinal cortex. Exp Brain Res 96:457–472.

Felleman DJ, Van Essen DC. 1991. Distributed hierarchical processing in the primate cerebral cortex. Cereb Cortex 1:1–47.

Funahashi S. 2006. Prefrontal cortex and working memory processes. Neuroscience 139:251–261.

Fuster JM. 2008. The prefrontal cortex. Amsterdam: Academic Press/Elsevier.

Fuster JM, Alexander GE. 1971. Neuron activity related to short-term memory. Science 173:652–654.

Fuster JM, Jervey JP. 1981. Inferotemporal neurons distinguish and retain behaviorally relevant features of visual stimuli. Science 212:952–955.

Gaffan D. 1994. Scene-specific memory for objects: a model of episodic memory impairment in monkeys with fornix transection. Journal of cognitive neuroscience 6(4):305–320.

Gaffan D, Eacott MJ. 1995. Uncinate fascicle section leaves delayed matching-to-sample intact, with both large and small stimulus sets. Exp Brain Res 105:175–180.

Gaffan D, Murray EA. 1992. Monkeys (*Macaca fascicularis*) with rhinal cortex ablations succeed in object discrimination learning despite 24-hr intertrial intervals and fail at matching to sample despite double sample presentations. Behav Neurosci 106:30–38.

Gerbella M, Belmalih A, Borra E, Rozzi S, Luppino G. 2010. Cortical connections of the macaque caudal ventrolateral prefrontal areas 45A and 45B. Cereb Cortex 20:141–168.

Gerbella M, Borra E, Tonelli S, Rozzi S, Luppino G. 2013. Connectional heterogeneity of the ventral part of the macaque area 46. Cereb Cortex 23(4):967–987.

Gloor P. 1997. The temporal lobe and limbic system. New York: Oxford University Press.

Goldman-Rakic PS. 1992. Working memory and the mind. Sci Am 267:110–117.

Goldman-Rakic PS, Selemon LD, Schwartz ML. 1984. Dual pathways connecting the dorsolateral prefrontal cortex with the hippocampal formation and parahippocampal cortex in the rhesus monkey. Neuroscience 12:719–743.

Horel JA. 1994. Retrieval of color and form during suppression of temporal cortex with cold. Behav Brain Res 65:165–172.

Horel JA, Pytko-Joiner DE, Voytko ML, Salsbury K. 1987. The performance of visual tasks while segments of the inferotemporal cortex are suppressed by cold. Behav Brain Res 23:29–42.

Hoshi E. 2006. Functional specialization within the dorsolateral prefrontal cortex: a review of anatomical and physiological studies of non-human primates. Neurosci Res 54: 73–84.

Insausti R. 2013. Comparative neuroanatomical parcellation of the human and nonhuman primate temporal pole. J Comp Neurol 521:4163–4176.

Insausti R, Amaral DG. 2008. Entorhinal cortex of the monkey: IV. Topographical and laminar organization of cortical afferents. J Comp Neurol 509:608–641.

Insausti R, Amaral DG. 2012. The hippocampal formation. In: Mai JK, Paxinos G, editors. The human nervous system, 3rd ed. Amsterdam: Elsevier Academic Press. p 896–942.

Insausti R, Amaral DG, Cowan WM. 1987. The entorhinal cortex of the monkey: II. Cortical afferents. J Comp Neurol 264:356–395.

Iversen SD, Mishkin M. 1970. Perseverative interference in monkeys following selective lesions of the inferior prefrontal convexity. Exp Brain Res 11:376–386.

Janssen P, Vogels R, Orban GA. 2000. Selectivity for 3D shape that reveals distinct areas within macaque inferior temporal cortex. Science 288:2054–2056.

Jellema T, Maassen G, Perrett DI. 2004. Single cell integration of animate form, motion and location in the superior temporal cortex of the macaque monkey. Cereb Cortex 14:781–790.

Jones EG, Powell TP. 1970. An anatomical study of converging sensory pathways within the cerebral cortex of the monkey. Brain 93:793–820.

Kaada BR. 1960. [Psychosomatic correlations elucidated by the stimulation and extirpation of central nervous structures]. Tidsskr Nor Laegeforen 80:181–197.

Kaada BR, Pribram KH, Epstein JA. 1949. Respiratory and vascular responses in monkeys from temporal pole, insula, orbital surface and cingulate gyrus; a preliminary report. J Neurophysiol 12:347–356.

Kawamura K, Naito J. 1984. Corticocortical projections to the prefrontal cortex in the rhesus monkey investigated with horseradish peroxidase techniques. Neurosci Res 1:89–103.

Klingler J, Gloor P. 1960. The connections of the amygdala and of the anterior temporal cortex in the human brain. J Comp Neurol 115:333–369.

Kluver H, Bucy PC. 1939. Preliminary analysis of functions of the temporal lobes in monkeys. J Neuropsychiatr Clin Neurosci 9:606–620.

Kobayashi Y, Amaral DG. 2007. Macaque monkey retrosplenial cortex: III. Cortical efferents. J Comp Neurol 502: 810–833.

Koechlin E, Summerfield C. 2007. An information theoretical approach to prefrontal executive function. Trends Cogn Sci 11:229–235.

Kondo H, Saleem KS, Price JL. 2003. Differential connections of the temporal pole with the orbital and medial prefrontal networks in macaque monkeys. J Comp Neurol 465: 499–523.

Kondo H, Saleem KS, Price JL. 2005. Differential connections of the perirhinal and parahippocampal cortex with the orbital and medial prefrontal networks in macaque monkeys. J Comp Neurol 493:479–509.

Kowalska DM, Bachevalier J, Mishkin M. 1991. The role of the inferior prefrontal convexity in performance of delayed nonmatching-to-sample. Neuropsychologia 29:583–600.

Kubota K, Suzuki H. 1973. Proceedings: 320. Visuokinetic neurons of the prefrontal cortex and delayed response. Nihon Seirigaku Zasshi 35:517.

Lavenex P, Suzuki WA, Amaral DG. 2002. Perirhinal and parahippocampal cortices of the macaque monkey: projections to the neocortex. J Comp Neurol 447:394–420.

Luebke J, Barbas H, Peters A. 2010. Effects of normal aging on prefrontal area 46 in the rhesus monkey. Brain Res Rev 62:212–232.

Luppino G, Matelli M, Camarda R, Rizzolatti G. 1993. Corticocortical connections of area F3 (SMA-proper) and area F6 (pre-SMA) in the macaque monkey. J Comp Neurol 338:114–140.

Markowitsch HJ, Emmans D, Irle E, Streicher M, Preilowski B. 1985. Cortical and subcortical afferent connections of the primate's temporal pole: a study of rhesus monkeys, squirrel monkeys, and marmosets. J Comp Neurol 242:425–458.

Martin-Elkins CL, Horel JA. 1992. Cortical afferents to behaviorally defined regions of the inferior temporal and parahippocampal gyri as demonstrated by WGA-HRP. J Comp Neurol 321:177–192.

Medalla M, Barbas H. 2014. Specialized prefrontal "auditory fields": organization of primate prefrontal-temporal pathways. Front Neurosci 8:1–15.

Meunier M, Bachevalier J, Mishkin M, Murray EA. 1993. Effects on visual recognition of combined and separate

ablations of the entorhinal and perirhinal cortex in rhesus monkeys. J Neurosci 13:5418–5432.

Mikami A, Ito S, Kubota K. 1982. Visual response properties of dorsolateral prefrontal neurons during visual fixation task. J Neurophysiol 47:593–605.

Miller EK, Desimone R. 1994. Parallel neuronal mechanisms for short-term memory. Science 263:520–522.

Miller EK, Li L, Desimone R. 1991. A neural mechanism for working and recognition memory in inferior temporal cortex. Science 254:1377–1379.

Miller EK, Li L, Desimone R. 1993. Activity of neurons in anterior inferior temporal cortex during a short-term memory task. J Neurosci 13:1460–1478.

Miyashita Y, Chang HS. 1988. Neuronal correlate of pictorial short-term memory in the primate temporal cortex. Nature 331:68–70.

Miyashita Y, Date A, Okuno H. 1993. Configurational encoding of complex visual forms by single neurons of monkey temporal cortex. Neuropsychologia 31:1119–1131.

Mohedano-Moriano A, Pro-Sistiaga P, Arroyo-Jimenez MM, Artacho-Perula E, Insausti AM, Marcos P, Cebada-Sanchez S, Martinez-Ruiz J, Munoz M, Blaizot X, Martinez-Marcos A, Amaral DG, Insausti R. 2007. Topographical and laminar distribution of cortical input to the monkey entorhinal cortex. J Anat 211:250–260.

Mohedano-Moriano A, Martinez-Marcos A, Pro-Sistiaga P, Blaizot X, Arroyo-Jimenez MM, Marcos P, Artacho-Perula E, Insausti R. 2008. Convergence of unimodal and polymodal sensory input to the entorhinal cortex in the fascicularis monkey. Neuroscience 151:255–271.

Moran MA, Mufson EJ, Mesulam MM. 1987. Neural inputs into the temporopolar cortex of the rhesus monkey. J Comp Neurol 256:88–103.

Morecraft RJ, Geula C, Mesulam MM. 1992. Cytoarchitecture and neural afferents of orbitofrontal cortex in the brain of the monkey. J Comp Neurol 323:341–358.

Morris R, Pandya DN, Petrides M. 1999. Fiber system linking the mid-dorsolateral frontal cortex with the retrosplenial/presubicular region in the rhesus monkey. J Comp Neurol 407:183–192.

Munoz DP, Everling S. 2004. Look away: the anti-saccade task and the voluntary control of eye movement. Nat Rev 5:218–228.

Munoz M, Insausti R. 2005. Cortical efferents of the entorhinal cortex and the adjacent parahippocampal region in the monkey (*Macaca fascicularis*). Eur J Neurosci 22: 1368–1388.

Murray EA, Davidson M, Gaffan D, Olton DS, Suomi S. 1989. Effects of fornix transection and cingulate cortical ablation on spatial memory in rhesus monkeys. Exp Brain Res 74:173–186.

Myers RE. 1972. Role of prefrontal and anterior temporal cortex in social behavior and affect in monkeys. Acta Neurobiol Exp 32:567–579.

Nakamura K, Kubota K. 1995. Mnemonic firing of neurons in the monkey temporal pole during a visual recognition memory task. J Neurophysiol 74:162–178.

Nakamura K, Matsumoto K, Mikami A, Kubota K. 1994. Visual response properties of single neurons in the temporal pole of behaving monkeys. J Neurophysiol 71:1206–1221.

Nauta WJ, Whitlock DG. 1956. Subcortical projections from the temporal neocortex in *Macaca mulatta*. J Comp Neurol 106:183–212.

Olson DA. 2003. Kluver-Bucy syndrome as a result of minor head trauma. South Med J 96:323.

Olson IR, Plotzker A, Ezzyat Y. 2007. The Enigmatic temporal pole: a review of findings on social and emotional processing. Brain 130:1718–1731.

Pandya DN, Kuypers HG. 1969. Cortico-cortical connections in the rhesus monkey. Brain Res 13:13–36.

Pandya DN, Yeterian EH. 1990. Prefrontal cortex in relation to other cortical areas in rhesus monkey: architecture and connections. Prog Brain Res 85:63–94.

Pandya DN, Dye P, Butters N. 1971. Efferent cortico-cortical projections of the prefrontal cortex in the rhesus monkey. Brain Res 31:35–46.

Passingham R. 1975. Delayed matching after selective prefrontal lesions in monkeys (*Macaca mulatta*). Brain Res 92:89–102.

Patterson K, Nestor PJ, Rogers TT. 2007. Where do you know what you know? The representation of semantic knowledge in the human brain. Nat Rev 8:976–987.

Paxinos G, Huang XF, Toga AW. 2000. The rhesus monkey brain in stereotaxic coordinates. San Diego, CA: Academic Press.

Petrides M, Pandya DN. 1984. Projections to the frontal cortex from the posterior parietal region in the rhesus monkey. J Comp Neurol 228:105–116.

Petrides M, Pandya DN. 1988. Association fiber pathways to the frontal cortex from the superior temporal region in the rhesus monkey. J Comp Neurol 273:52–66.

Petrides M, Pandya DN. 1999. Dorsolateral prefrontal cortex: comparative cytoarchitectonic analysis in the human and the macaque brain and corticocortical connection patterns. Eur J Neurosci 11:1011–1036.

Petrides M, Pandya DN. 2002. Comparative cytoarchitectonic analysis of the human and the macaque ventrolateral prefrontal cortex and corticocortical connection patterns in the monkey. Eur J Neurosci 16:291–310.

Petrides M, Pandya DN. 2009. Distinct parietal and temporal pathways to the homologues of Broca's area in the monkey. PLoS Biol 7:e1000170.

Petrides M, Tomaiuolo F, Yeterian EH, Pandya DN. 2012. The prefrontal cortex: comparative architectonic organization in the human and the macaque monkey brains. Cortex 48:46–57.

Phillips RR, Malamut BL, Bachevalier J, Mishkin M. 1988. Dissociation of the effects of inferior temporal and limbic lesions on object discrimination learning with 24-h intertrial intervals. Behav Brain Res 27:99–107.

Rempel-Clower NL, Barbas H. 2000. The laminar pattern of connections between prefrontal and anterior temporal cortices in the Rhesus monkey is related to cortical structure and function. Cereb Cortex 10:851–865.

Riches IP, Wilson FA, Brown MW. 1991. The effects of visual stimulation and memory on neurons of the hippocampal formation and the neighboring parahippocampal gyrus and inferior temporal cortex of the primate. J Neurosci 11:1763–1779.

Ringo JL, Sobotka S, Diltz MD, Bunce CM. 1994. Eye movements modulate activity in hippocampal, parahippocampal, and inferotemporal neurons. J Neurophysiol 71:1285–1288.

Rizzolatti G, Luppino G. 2001. The cortical motor system. Neuron 31:889–901.

Rodman HR. 1994. Development of inferior temporal cortex in the monkey. Cereb Cortex 4:484–498.

Rodman HR, Consuelos MJ. 1994. Cortical projections to anterior inferior temporal cortex in infant macaque monkeys. Vis Neurosci 11:119–133.

Saleem KS, Logothetis KN. 2012. Atlas of the Rhesus monkey brain. In stereotaxic coordinates, 2nd ed. Amsterdam: Elsevier/Academic Press.

Saleem KS, Tanaka K. 1996. Divergent projections from the anterior inferotemporal area TE to the perirhinal and entorhinal cortices in the macaque monkey. J Neurosci 16:4757–4775.

Saleem KS, Price JL, Hashikawa T. 2007. Cytoarchitectonic and chemoarchitectonic subdivisions of the perirhinal and parahippocampal cortices in macaque monkeys. J Comp Neurol 500:973–1006.

Saleem KS, Miller B, Price JL. 2014. Subdivisions and connectional networks of the lateral prefrontal cortex in the macaque monkey. J Comp Neurol 522:1641–1690.

Selemon LD, Goldman-Rakic PS. 1988. Common cortical and subcortical targets of the dorsolateral prefrontal and posterior parietal cortices in the rhesus monkey: evidence for a distributed neural network subserving spatially guided behavior. J Neurosci 8:4049–4068.

Seltzer B, Pandya DN. 1978. Afferent cortical connections and architectonics of the superior temporal sulcus and surrounding cortex in the rhesus monkey. Brain Res 149:1–24.

Seltzer B, Pandya DN. 1989. Frontal lobe connections of the superior temporal sulcus in the rhesus monkey. J Comp Neurol 281:97–113.

Shiwa T. 1987. Corticocortical projections to the monkey temporal lobe with particular reference to the visual processing pathways. Arch Ital Biol 125:139–154.

Suzuki H, Azuma M. 1983. Topographic studies on visual neurons in the dorsolateral prefrontal cortex of the monkey. Exp Brain Res 53:47–58.

Suzuki WA, Amaral DG. 1994a. Perirhinal and parahippocampal cortices of the macaque monkey: cortical afferents. J Comp Neurol 350:497–533.

Suzuki WA, Amaral DG. 1994b. Topographic organization of the reciprocal connections between the monkey entorhinal cortex and the perirhinal and parahippocampal cortices. J Neurosci 14:1856–1877.

Suzuki WA, Amaral DG. 2003. Perirhinal and parahippocampal cortices of the macaque monkey: cytoarchitectonic and chemoarchitectonic organization. J Comp Neurol 463:67–91.

Szabo J, Cowan WM. 1984. A stereotaxic atlas of the brain of the cynomolgus monkey (*Macaca fascicularis*). J Comp Neurol 222:265–300.

Takahashi E, Ohki K, Kim DS. 2013. Dissociation and convergence of the dorsal and ventral visual working memory streams in the human prefrontal cortex. NeuroImage 65: 488–498.

Tanji J, Hoshi E. 2008. Role of the lateral prefrontal cortex in executive behavioral control. Physiol Rev 88:37–57.

Ungerleider LG, Gaffan D, Pelak VS. 1989. Projections from inferior temporal cortex to prefrontal cortex via the uncinate fascicle in rhesus monkeys. Exp Brain Res 76:473–484.

Van Hoesen GW, Pandya DN. 1975. Some connections of the entorhinal (area 28) and perirhinal (area 35) cortices of the rhesus monkey. III. Efferent connections. Brain Res 95:39–59.

Van Hoesen G, Pandya DN, Butters N. 1975. Some connections of the entorhinal (area 28) and perirhinal (area 35) cortices of the rhesus monkey. II. Frontal lobe afferents. Brain Res 95:25–38.

van Kesteren MT, Ruiter DJ, Fernandez G, Henson RN. 2012. How schema and novelty augment memory formation. Trends Neurosci 35:211–219.

von Bonin G, Bailey P. 1947. The neocortex of *Macaca mulatta*. Urbana, IL: University of Illinois Press.

Walker AE. 1940. A cytoarchitectural study of the prefrontal area of the macaque monkey. J Comp Neurol 73:59–86.

Webster MJ, Bachevalier J, Ungerleider LG. 1994. Connections of inferior temporal areas TEO and TE with parietal and frontal cortex in macaque monkeys. Cereb Cortex 4: 470–483.

Weller RE, Kaas JH. 1987. Subdivisions and connections of inferior temporal cortex in owl monkeys. J Comp Neurol 256:137–172.

Weller RE, Steele GE. 1992. Cortical connections of subdivisions of inferior temporal cortex in squirrel monkeys. J Comp Neurol 324:37–66.

Weller RE, LeDoux MS, Toll LM, Gould MK, Hicks RA, Cox JE. 2006. Subdivisions of inferior temporal cortex in squirrel monkeys make dissociable contributions to visual learning and memory. Behav Neurosci 120:423–446.

Yeterian EH, Pandya DN, Tomaiuolo F, Petrides M. 2012. The cortical connectivity of the prefrontal cortex in the monkey brain. Cortex 48:58–81.

Zola-Morgan S, Squire LR, Clower RP, Rempel NL. 1993. Damage to the perirhinal cortex exacerbates memory impairment following lesions to the hippocampal formation. J Neurosci 13:251–265.